14. Morakkabati-Spitz N, Gieseke J, Kuhl C, et al. 3.0 T high-field magnetic resonance imaging of the female pelvis: preliminary experiences. Eur Radiol 2005;15:639–644.
15. Morakkabati-Spitz N, Schild HH, Kuhl CK, et al. Female pelvis: MR imaging at 3.0 T with sensitivity encoding and flip-angle sweep technique. Radiology 2006;241:538–545.
16. Morakkabati-Spitz N, Gieseke J, Kuhl C, et al. MRI of the pelvis at 3 T: very high spatial resolution with sensitivity encoding and flip-angle sweep technique in clinically acceptable scan time. Eur Radiol 2006;16:634–641.
17. Kataoka M, Kido A, Koyama T, et al. MRI of the female pelvis at 3T compared to 1.5T: evaluation on high-resolution T2-weighted and HASTE images. J Magn Reson Imaging 2007;25:527–534.
18. Torricelli P, Ferraresi S, Fiocchi F, et al. 3 T MRI in the preoperative evaluation of depth of myometrial infiltration in endometrial cancer. AJR Am J Roentgenol 2008;190:489–495.
19. Hori M, Kim T, Murakami T, et al. Uterine cervical carcinoma: preoperative staging with 3.0 T MR imaging — comparison with 1.5 T MR imaging. Radiology 2009;251:96–104.
20. Piver MS, Rutledge F, Smith JP. Five classes of extended hysterectomy for women with cervical cancer. Obstet Gynecol 1974;44:265–272.
21. Schmitt M, Feiweier T, Horger W, et al. Improved uniformity of RF-distribution in clinical whole body-imaging at 3T by means of dielectric pads. In: Proc 12th Annual Meeting ISMRM, Kyoto; 2004: 197.
22. Yang QX, Mao W, Wang J, et al. Manipulation of image intensity distribution at 7.0 T: passive RF shimming and focusing with dielectric materials. J Magn Reson Imaging 2006;24:197–202.
23. Heverhagen JT. Noise measurement and estimation in MR imaging experiments. Radiology 2007;245:638–639.
24. Landis JR, Koch GG. The measurement of observer agreement for categorical data. Biometrics 1977;33:159–174.
25. Gibbs GF, Huston J 3rd, Bernstein MA, Riederer SJ, Brown RD Jr. Improved image quality of intracranial aneurysms: 3.0 T versus 1.5 T time-of-flight MR angiography. AJNR Am J Neuroradiol 2004;25: 84–87.
26. Kuhl CK, Textor J, Gieseke J, et al. Acute and subacute ischemic stroke at high-field-strength (3.0 T) diffusion-weighted MR imaging: intraindividual comparative study. Radiology 2005;234:509–516.
27. Norris DG. High field human imaging. J Magn Reson Imaging 2003;18:519–529.
28. Schick F. Whole-body MRI at high field: technical limits and clinical potential. Eur Radiol 2005;15:946–959.
29. Bottomley PA, Foster TH, Argersinger RE, et al. A review of normal tissue hydrogen NMR relaxation times and relaxation mechanisms from 1-100 MHz: dependence on tissue type, NMR frequency, temperature, species, excision, and age. Med Phys 1984;11:425–448.
30. de Bazelaire CM, Duhamel GD, Rofsky NM, Alsop DC. MR imaging relaxation times of abdominal and pelvic tissues measured in vivo at 3.0 T: preliminary results. Radiology 2004;230:652–659.
31. Kuhl CK, Träber F, Schild HH. Whole-body high-field-strength (3.0 T) MR imaging in clinical practice. Part I. Technical considerations and clinical applications. Radiology 2008;246:675–696.
32. Nöbauer-Huhmann IM, Ba-Ssalamah A, Mlynarik V, et al. Magnetic resonance imaging contrast enhancement of brain tumors at 3 Tesla versus 1.5 Tesla. Invest Radiol 2002;37:114–119.
33. Kuhl CK, Jost P, Morakkabati N, Zivanovic O, Schild HH, Gieseke J. Contrast-enhanced MR imaging of the breast at 3.0 and 1.5 T in the same patients: initial experience. Radiology 2006;239:666–676.
34. Zhu Y. Parallel excitation with an array of transmit coils. Magn Reson Med 2004;51:775–784.
35. Van den Berg CA, van den Bergen B, Van de Kamer JB, et al. Simultaneous B1+ homogenization and specific absorption rate hotspot suppression using a magnetic resonance phased array transmit coil. Magn Reson Med 2007;57:577–586.

# Uterine Cervical Carcinoma: Preoperative Staging with 3.0-T MR Imaging—Comparison with 1.5-T MR Imaging[1]

Masatoshi Hori, MD, PhD
Tonsok Kim, MD
Takamichi Murakami, MD, PhD
Izumi Imaoka, MD, PhD
Hiromitsu Onishi, MD, PhD
Kaname Tomoda, MD, PhD
Tateki Tsutsui, MD, PhD
Takayuki Enomoto, MD, PhD
Tadashi Kimura, MD, PhD
Hironobu Nakamura, MD, PhD

**Purpose:** To prospectively evaluate the efficacy of 3.0-T magnetic resonance (MR) imaging in the preoperative staging of cervical carcinoma compared with that at 1.5-T imaging, with surgery and pathologic analysis as the reference standards.

**Materials and Methods:** Institutional review board approval and informed consent were obtained. Thirty-one consecutive patients (age range, 27–71 years; mean age, 51.1 years) underwent 3.0- and 1.5-T MR imaging. Quantitative and qualitative analyses were performed. Two radiologists independently evaluated images in terms of local-regional staging. MR findings were compared with surgicopathologic findings.

**Results:** Mean tumor signal-to-noise ratios, mean cervical stroma signal-to-noise ratios, and mean tumor-to–cervical stroma contrast-to-noise ratios at 3.0-T imaging were significantly higher than those at 1.5-T imaging ($P = 9.1 \times 10^{-6}$, $P = 1.8 \times 10^{-6}$, and $P = .008$, respectively). Image homogeneity at 3.0-T imaging was significantly inferior to that at 1.5-T imaging ($P = .005$). There were no significant differences in terms of the degree of susceptibility artifacts. Interobserver agreement between the two radiologists for local-regional staging was good or excellent ($\kappa = 0.65$–$0.89$). Sensitivity, specificity, and area under the receiver operating characteristic curve for radiologist 1 in the evaluation of parametrial invasion were *(a)* 75% for both 3.0- and 1.5-T imaging, *(b)* 70% for both 3.0- and 1.5-T imaging, and *(c)* 0.82 for 3.0-T imaging and 0.85 for 1.5-T imaging, respectively. Corresponding values for vaginal invasion were *(a)* 67% for both 3.0- and 1.5-T imaging, *(b)* 68% for 3.0-T imaging and 72% for 1.5-T imaging, and *(c)* 0.62 for 3.0-T imaging and 0.67 for 1.5-T imaging, respectively. Corresponding values for lymph node metastases were *(a)* 57% for both 3.0- and 1.5-T imaging, *(b)* 83% for 3.0-T imaging and 88% for 1.5-T imaging, and *(c)* 0.72 for 3.0-T imaging and 0.78 for 1.5-T imaging, respectively. Neither radiologist noted significant differences between values obtained with 3.0-T imaging and those obtained with 1.5-T imaging ($P > .5$ for all comparison pairs).

**Conclusion:** In this study, 3.0-T MR imaging was characterized by high diagnostic accuracy in the presurgical evaluation of patients with cervical carcinoma, although 3.0-T imaging was not significantly superior to 1.5-T imaging.



[1] From the Departments of Radiology (M.H., T. Kim, H.O., K.T., H.N.) and Obstetrics and Gynecology (T.T., T.E., T. Kimura), Osaka University Graduate School of Medicine, D1, 2-2, Yamadaoka, Suita, Osaka 565-0871, Japan; and Department of Radiology, Kinki University School of Medicine, Osaka, Japan (T.M., I.I.). Received July 21, 2008; revision requested August 30; revision received September 9; accepted September 29; final version accepted October 13. **Address correspondence to** M.H. (e-mail: *mhori@radiol.med.osaka-u.ac.jp*).

Carcinoma of the uterine cervix is the third most common gynecologic malignancy in the United States, with an estimated 11 070 new cases of this cancer and an estimated 3870 deaths from this disease in 2008 (1). Over the past several decades, the mortality rate has decreased as a result of screening with the Papanicolaou test; however, the survival rate of patients with invasive carcinomas has remained unchanged (2–5). Cervical carcinoma is usually staged and managed on the basis of criteria proposed by the International Federation of Gynecology and Obstetrics (FIGO). These criteria take into account the physical examination, colposcopy, chest radiography, excretory urography, cystoscopy, proctosigmoidoscopy, and barium enema examination findings. However, the FIGO staging system is sometimes inaccurate, in spite of the fact that accurate staging is essential for appropriate treatment planning (5–7). The usefulness of magnetic resonance (MR) imaging in the preoperative assessment of patients with cervical carcinoma has been recognized (7–13) and is expected to optimize the therapeutic strategy.

Theoretically, 3.0-T MR imaging offers a higher signal-to-noise ratio (SNR) and higher spectral separation than does 1.5-T MR imaging. While 3.0-T imaging has already been shown to be more effective than 1.5-T imaging in the brain and musculoskeletal system, the advantages of its use in the abdomen or pelvis remain unclear because of artifacts like dielectric effects (14,15). Since these artifacts can deteriorate image quality and potentially lead to inferior diagnostic capability, 3.0-T MR imaging may not be adequate for use in the preoperative assessment of cervical carcinoma. This could be a major problem in view of the fact that the number of 3.0-T MR imagers is increasing worldwide. Although some reports have dealt with the value of 3.0-T imaging in the examination of the female pelvis (16–20), to our knowledge, no one has investigated the efficacy of 3.0-T imaging in the presurgical evaluation of cervical carcinoma. Thus, the purpose of our study was to prospectively evaluate the efficacy of 3.0-T MR imaging in the preoperative staging of cervical carcinoma compared with that at 1.5-T imaging, with surgery and pathologic analysis as the reference standards.

## Advances in Knowledge

- The tumor signal-to-noise ratio of 3.0-T MR imaging was 15% better than that of 1.5-T MR imaging.
- Image homogeneity of 3.0-T MR imaging was inferior to that of 1.5-T MR imaging ($P = .005$).
- Susceptibility artifacts on 3.0-T MR images were larger than those on 1.5-T MR images, but this difference was not significant ($P = .11$).
- The diagnostic capability of 3.0-T MR imaging in the presurgical evaluation of cervical carcinoma was good and comparable to that of state-of-the-art 1.5-T MR imaging.

## Materials and Methods

### Patients

This study was approved by the Osaka University Hospital institutional review board, and written informed consent was obtained from all patients. Between November 2006 and October 2007, 59 consecutive women with biopsy-proved untreated cervical carcinoma were examined with MR imaging at Osaka University Hospital. Of these patients, 16 did not agree to be included in the study, and 12 underwent radiation therapy and were excluded from the study. Thus, the final study population comprised 31 patients (age range, 27–71 years; mean age, 51.1 years ± 9.8 [standard deviation]). All of the patients underwent surgery 13–75 days (mean, 33.5 days ± 15.1) after MR examination. Surgical confirmation of the diagnosis was obtained by means of Piver type IV hysterectomy with pelvic lymphadenectomy in 27 patients, Piver type III hysterectomy with pelvic lymphadenectomy in one patient, abdominal radical trachelectomy with pelvic lymphadenectomy in two patients, and total vaginal hysterectomy in one patient (21). Histologic examination enabled us to establish that of the 31 tumors, 22 (71%) were squamous cell carcinomas, four (13%) were mucinous adenocarcinomas, two (6%) were serous adenocarcinomas, two (6%) were endometrioid adenocarcinomas, and one (3%) was an adenosquamous cell carcinoma. Pathologic examination demonstrated stage IA1 disease in two patients, stage IA2 disease in one patient, stage IB1 disease in 17 patients, stage IB2 disease in three patients, stage IIA disease in four patients, and stage IIB disease in four patients. One patient did not undergo pelvic lymphadenectomy, and we presumed that this patient did not have metastatic

## Implications for Patient Care

- MR imaging at 3.0 T is an effective diagnostic modality in the presurgical evaluation of patients with cervical cancer because its diagnostic performance is comparable to that of state-of-the-art 1.5-T imaging.
- Because image homogeneity due to insufficient radiofrequency penetration at 3.0-T imaging is inferior to that at 1.5-T imaging, it may be advisable to use 1.5-T MR imaging to evaluate certain kinds of patients, such as those who are obese or have massive ascites.

**Published online before print**
10.1148/radiol.2511081265

**Radiology 2009; 251:96–104**

**Abbreviations:**
CNR = contrast-to-noise ratio
SNR = signal-to-noise ratio

**Author contributions:**
Guarantor of integrity of entire study, M.H.; study concepts/study design or data acquisition or data analysis/interpretation, all authors; manuscript drafting or manuscript revision for important intellectual content, all authors; manuscript final version approval, all authors; literature research, M.H., T. Kim, T.M., I.I.; clinical studies, M.H., T. Kim, H.O., K.T., T.T., T.E., T. Kimura, H.N.; experimental studies, M.H., I.I., H.O.; statistical analysis, M.H.; and manuscript editing, all authors

Authors stated no financial relationship to disclose.

lymph nodes on the basis of preoperative computed tomography (CT) and MR findings and follow-up CT findings obtained 6 months after surgery.

### MR Examination

MR imaging was performed with state-of-the-art 3.0- and 1.5-T imagers (Signa Excite HD 3.0 T and Signa Excite HD 1.5 T; GE Healthcare, Milwaukee, Wis) operating with comparable software and eight-channel body-array coils. For 3.0-T MR imaging, a dielectric pad was placed on the patient's body to improve image homogeneity (22,23). After acquisition of localization images, T2-weighted fast spin-echo images were obtained in oblique sagittal (parasagittal) planes that were parallel to the longitudinal axis of the cervical canal, as well as in oblique (paraxial or paracoronal) planes that were vertical to the cervical canal. The imaging parameters were as follows: repetition time msec/echo time msec, 6000/90 for 3.0-T imaging and 4000/90 for 1.5-T imaging; two signals acquired; echo train length, 18 for 3.0-T imaging and 12 for 1.5-T imaging; receiver bandwidth, 62.5 kHz for 3.0-T imaging and 31.2 kHz for 1.5-T imaging; and 512 × 256 matrix. The section thickness was 5 mm, with a 1-mm intersection gap and a 24-cm field of view. Imaging was performed with superior and inferior spatial presaturation pulses. Saturation bands were placed anteriorly for imaging in parasagittal planes to eliminate the phase-shift artifacts caused by subcutaneous fat. If prominent artifacts from subcutaneous fat were observed in the paraxial plane, we planned to perform additional T2-weighted imaging in this plane with an anterior saturation band. However, this was not needed in our series. Sensitivity encoding techniques were not used. Acquisition time was 198 seconds for 3.0-T imaging and 184 seconds for 1.5-T imaging for each T2-weighted sequence. We performed 3.0- and 1.5-T MR imaging on the same day within a 30-minute interval, and the order of imaging (whether the patient underwent 3.0- or 1.5-T MR imaging first) was random. Fifteen patients underwent the 3.0-T study first, and the remaining 16 patients underwent the 1.5-T study first. Except when contraindicated, 20 mg of butyl-scopolamine (Buscopan; Nippon Boehringer Ingelheim, Tokyo, Japan) was administered intramuscularly to all patients before the examination to prevent peristalsis artifacts. After T2-weighted images were acquired with both 3.0- and 1.5-T imagers, unenhanced T1-weighted and contrast material–enhanced (17 mL of gadoteridol; ProHance, Eisai, Tokyo, Japan) dynamic T1-weighted MR images were obtained with the 3.0- or 1.5-T imager; however, these images were not used in our study.

### Image Analysis

*Quantitative analysis.*—All images were transferred to a workstation (Advantage Workstation 4.2; GE Healthcare) for quantitative analysis. One radiologist (M.H., 15 years experience in genitourinary imaging) performed the analysis and, whenever possible, applied it to images by using the operator-defined region-of-interest (ROI) measurements of mean signal intensity in the cervical stroma (mean area, 0.3 $cm^2$ ± 0.1; range, 0.1–0.6 $cm^2$) and tumors (mean area, 3.4 $cm^2$ ± 3.1; range, 0.3–12.0 $cm^2$). Signal intensity was measured in areas devoid of focal signal intensity changes and prominent artifacts. For tumors, a circular ROI was drawn as large as possible to encompass as much of the lesion as possible. The standard deviation of background noise ($SD_B$) was measured along the phase-encoding direction outside the anterior abdominal wall (mean ROI size, 13.4 $cm^2$ ± 3.6; range, 3.8–16.2 $cm^2$) to calculate *(a)* tumor SNR ($SNR_T$) with the equation $SNR_T = SI_T/SD_B$, *(b)* cervical stroma SNR ($SNR_{CS}$) with the equation $SNR_{CS} = SI_S/SD_B$, and *(c)* tumor-to-cervical stroma contrast-to-noise ratio (CNR) with the equation $CNR = (SI_T - SI_S)/SD_B$, where $SI_T$ is the signal intensity of the tumor and $SI_S$ is the signal intensity of the cervical stroma.

*Image qualitative analysis.*—Another radiologist (T.Kim, 18 years of experience in genitourinary imaging) reviewed the images obtained in both oblique planes with the 3.0- and 1.5-T units. This review was conducted over the course of two sessions separated by a 2-week interval, with one set of images from each subject reviewed during each session. The order of the patients was randomized, as was the order in which images obtained with either the 3.0-T unit or the 1.5-T unit were reviewed. To minimize bias, the patient name, imaging parameters, and MR unit used for imaging were masked. The radiologist graded images in terms of image homogeneity and susceptibility artifacts with a four-point scale (1, unacceptable; 2, poor; 3, fair; and 4, good).

*Diagnostic performance analysis.*—Two radiologists (T.Kim, I.I.) with more than 15 years of experience in gynecologic MR imaging independently reviewed the images obtained with the 3.0- and 1.5-T units. One of the radiologists (I.I.) was from another hospital and was invited to review the images. This radiologist was not involved in the prospective clinical care of any of these patients. The other radiologist (T.Kim) was involved in the clinical care of some of these patients. T2-weighted images obtained in both oblique planes were reviewed. This review was conducted over the course of two sessions separated by a 2-week interval in the same manner as the image quality analysis. The reviewers were blinded to the histopathologic findings, patient name, imaging parameters, and MR unit used; however, they were aware of the patient's age. There was no time restriction for reviewing the images for each case.

The readers were asked to score the images obtained in each patient for the presence of parametrial invasion, vaginal invasion, and lymph node metastases. The readers rated the images and assigned a confidence level (1, definitely absent; 2, probably absent; 3, equivocal; 4, probably present; and 5, definitely present). For calculation of sensitivity and specificity, confidence levels of 1, 2, and 3 were classified as negative, whereas confidence levels of 4 and 5 were classified as positive. These assessments were made on the basis of established MR criteria. First, patients

with supravaginal tumors were suspected of having parametrial invasion if disruption of the hypointense stroma and protrusion through the disrupted stroma into the parametrium were observed. Preservation of the hypointense stromal ring on T2-weighted images was considered a sign of intact parametrium. Patients with tumors within the vaginal fornix were suspected of having parametrial invasion when the lesion protruded through the defect of the hypointense thin vaginal fornix. Vaginal invasion was diagnosed when segmental disruption of a low-signal-intensity vagina or a thick hyperintense vagina was observed. Lymph node metastasis was diagnosed when enlarged regional lymph nodes with a minimal diameter larger than 1 cm were identified.

### Statistical Analyses

The paired *t* test was used to compare SNRs and CNRs on 3.0- and 1.5-T images. The Wilcoxon signed rank test was used for statistical comparison of image quality scores.

**Figure 1**

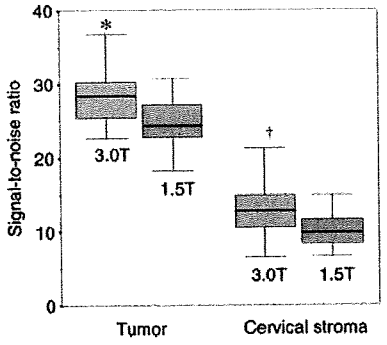


**Figure 1:** Box plots show SNRs of tumors and cervical stroma. Box plots indicate the median (horizontal line), the 75th (top of box) and 25th (bottom of box) quartiles, and the smallest and largest nonextreme values (whiskers). Mean values were significantly higher for 3.0-T imaging than for 1.5-T imaging for tumors and cervical stroma. The mean ratio of SNR at 3.0-T imaging to that at 1.5-T imaging was 1.15 for tumors and 1.24 for cervical stroma. The signal intensity of tumors was measured in 21 patients, and the signal intensity of cervical stroma was measured in 29 patients. *P* values were calculated with the paired *t* test. * = $P = 9.1 \times 10^{-6}$. † $P = 1.8 \times 10^{-6}$.

MR findings were compared with surgicopathologic findings. Sensitivity, specificity, positive and negative predictive values, and diagnostic accuracy of the 3.0- and 1.5-T MR imagers were calculated for diagnosis of parametrial invasion, vaginal invasion, and lymph node metastases. These diagnostic parameters were expressed with a 95% confidence interval. The McNemar test was used for statistical comparison of sensitivity and specificity. Receiver operating characteristic analysis was performed to evaluate diagnostic performance in relation to parametrial invasion, vaginal invasion, and lymph node metastases. A receiver operating characteristic curve was fitted to each reader's confidence rating by using a maximum likelihood estimation program (ROCKIT, version 0.9B; C. E. Metz, University of Chicago, Chicago, Ill). The diagnostic performance was then estimated by calculating the area under the receiver operating characteristic curve. The univariate *z* score was calculated to evaluate the significance of the difference between the area under the receiver operating characteristic curve values.

Regarding the five-point scale used to evaluate diagnostic performance, interobserver agreement between the two readers and intermodality agreement between the 3.0- and 1.5-T imager were determined by calculating the weighted κ values (quadratic weighting), with a κ value of 0.00 indicating poor agreement; 0.01–0.20, slight agreement; 0.21–0.40, fair agreement; 0.41–0.60, moderate agreement; 0.61–0.80, good agreement; and 0.81–1.00, excellent agreement (24).

For all statistical analyses other than receiver operating characteristic analysis, a software package (SPSS for Windows, version 11.0; SPSS, Chicago, Ill) was used. A two-tailed *P* value of less than .05 was considered to indicate a significant difference. Power analysis indicated that a minimum sample size of 12 patients would provide 80% power and a 5% significance level in the detection of a mean difference of 15% between values at 3.0- and 1.5-T imaging in tumor SNR, cervical stromal SNR, and tumor-to–cervical stroma CNR. Since our study was an initial experience, no power analysis was performed in terms of diagnostic performance evaluation.

**Figure 2**

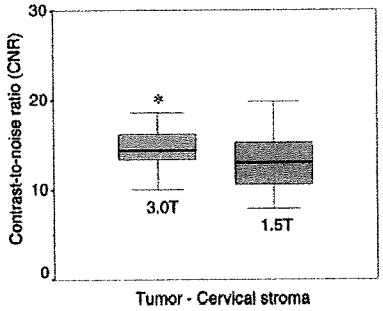


**Figure 2:** Box plots show tumor-to–cervical stroma CNR. The tumor-to–cervical stroma CNR was calculated in 19 patients. Box plots indicate the median (horizontal line), the 75th (top of box) and 25th (bottom of box) quartiles, and the smallest and largest nonextreme values (whiskers). The mean ratio of tumor-to–cervical stroma CNR at 3.0-T imaging to that at 1.5-T imaging was 1.16. Mean values were significantly higher for 3.0-T imaging than for 1.5-T imaging. * = *P* = .008 (paired *t* test).

## Results

### Quantitative Analysis

On 3.0- and 1.5-T images, tumors could barely be identified in 10 subjects mainly because the tumors were small, and cervical stroma could not be clearly observed in two patients. Thus, signal intensity was obtained for tumors in 21 patients and for cervical stroma in 29 patients, whereas tumor-to–cervical stroma CNR was obtained in 19 patients. The mean SNR of tumors ($P = 9.1 \times 10^{-6}$), mean SNR of cervical stroma ($P = 1.8 \times 10^{-6}$), and mean tumor-to–cervical stroma CNR ($P = .008$) at 3.0-T imaging were significantly higher than those at 1.5-T imaging (Figs 1–3). The mean ratio of SNR at 3.0-T imaging to SNR at 1.5-T imaging was 1.15 (95% confidence interval: 1.10, 1.20) for tumors and 1.24 (95% confidence interval: 1.15, 1.33) for cervical stroma. The mean ratio of

tumor-to-stroma CNR at 3.0-T imaging to that at 1.5-T imaging was 1.16 (95% confidence interval: 1.04, 1.27).

### Image Qualitative Analysis

Two patients had poor image homogeneity at 3.0-T imaging, whereas no patient had poor image homogeneity at 1.5-T imaging. The score for image homogeneity at 3.0-T imaging was significantly inferior to that at 1.5-T imaging ($P = .005$) (Table 1; Figs 3, 4). The score for susceptibility artifacts at 3.0-T imaging was also inferior to that at 1.5-T imaging; however, this difference was not significant ($P = .11$).

### Diagnostic Performance Analysis

There were no significant differences between 3.0- and 1.5-T MR imaging in terms of the area under the receiver operating characteristic curve, sensitivity, or specificity for each reader ($P > .5$ for all comparison pairs) (Table 2; Figs 4, 5). There was excellent interobserver and intermodality agreement for the diagnosis of parametrial invasion and lymph node metastases ($\kappa > 0.80$) (Table 3) and good interobserver and intermodality agreement for the diagnosis of vaginal invasion ($\kappa = 0.65–0.77$).

## Discussion

The SNR at 3.0-T imaging can theoretically be expected to be twice as high as that at 1.5-T imaging. This higher SNR can be maintained or traded for greater speed, improved spatial resolution, or both. Thus, the use of 3.0-T imaging has been firmly established in the neuroradiologic field (25,26); however, there are many problems associated with 3.0-T imaging, particularly imaging of the abdomen and pelvis. These problems include *(a)* increased T1 relaxation time and somewhat shortened T2 relaxation time, *(b)* larger chemical shift, *(c)* larger susceptibility effect, *(d)* radiofrequency inhomogeneity, *(e)* increased power deposition, and *(f)* uncertain efficacy of contrast agents (14,27–29). As a result, the advantages of a higher magnetic field are not directly applicable to the chest, abdomen, or pelvis. Our re-

**Figure 3**

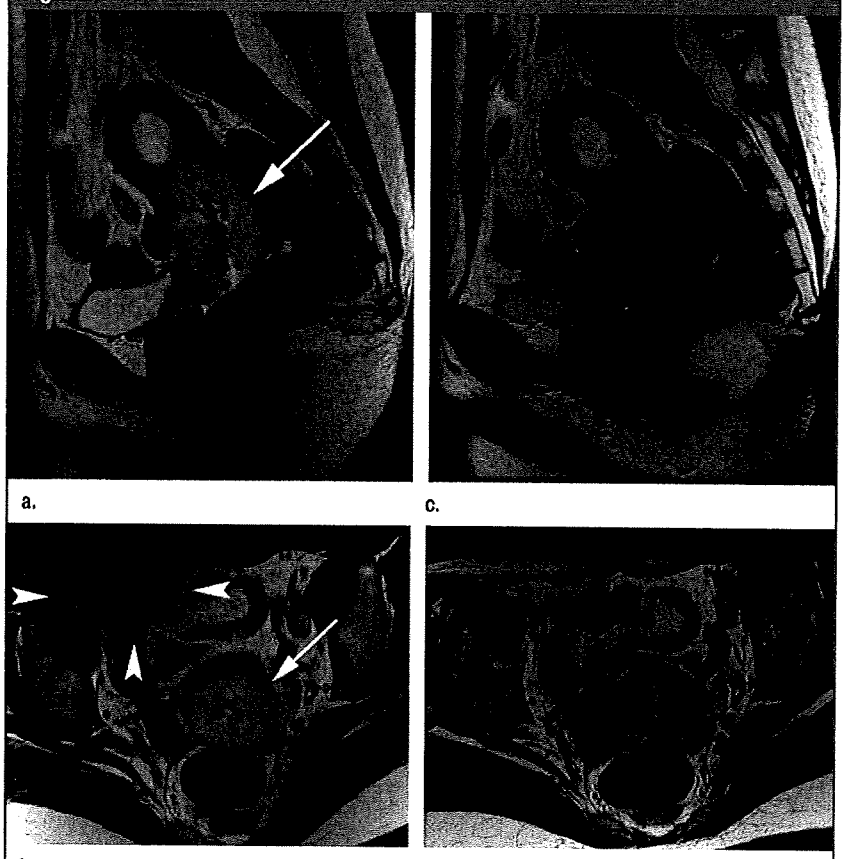


**Figure 3:** T2-weighted fast spin-echo MR images in a 57-year-old woman with cervical carcinoma (squamous cell carcinoma, nonkeratinizing type, pT1b2). Oblique 3.0-T images (6000/90; echo train length, 18) in the **(a)** parasagittal and **(b)** paraxial planes of the uterus clearly show the tumor (arrow). Oblique 1.5-T images (4000/90; echo train length, 12) in the **(c)** parasagittal and **(d)** paraxial planes of the uterus show the tumor with somewhat reduced signal intensity. Signal intensity of the tumor is higher at 3.0-T imaging than at 1.5-T imaging, while image homogeneity is slightly better with 1.5-T imaging than with 3.0-T imaging. Signal loss artifact (arrowheads in **b**) due to radiofrequency inhomogeneity is seen on 3.0-T images.

**Table 1**

**Results of Scores for Image Quality with 3.0- and 1.5-T MR Imaging in 31 Patients**

| Score | Image Homogeneity* | | Susceptibility Artifact† | |
|---|---|---|---|---|
| | 3.0-T Imaging | 1.5-T Imaging | 3.0-T Imaging | 1.5-T Imaging |
| 4 | 9 (29) | 19 (61) | 12 (39) | 19 (61) |
| 3 | 20 (65) | 12 (39) | 19 (61) | 12 (39) |
| 2 | 2 (6) | 0 (0) | 0 (0) | 0 (0) |
| 1 | 0 (0) | 0 (0) | 0 (0) | 0 (0) |

Note.—Data in parentheses are percentages. Image quality was graded in terms of homogeneity and susceptibility artifacts with the aforementioned four-point scale. *P* values were calculated with the Wilcoxon signed rank test for statistical comparison of scores at 3.0- and 1.5-T MR imaging.

* $P = .005$.

† $P = .11$.

sults show that 3.0-T imaging can improve tumor SNR by approximately 15% and tumor-to-stroma CNR by approximately 16%, yield inferior image homogeneity, and have equivalent diagnostic capability for the presurgical evaluation of cervical carcinoma compared with state-of-the-art 1.5-T MR imaging. This means that 3.0-T imaging is an effective diagnostic modality in the presurgical evaluation of patients with cervical cancer.

The evaluation of parametrial invasion is important because it greatly influences therapeutic strategy. Radiation therapy alone or in combination with chemotherapy is the preferred treatment for stage IIB or higher cancer and for lesions larger than 4 cm in diameter, whereas surgery is the treatment of choice for lower-stage disease. Our results show a high negative predictive value of 95% for both 3.0- and 1.5-T imaging in terms of parametrial invasion and high sensitivity, specificity, and accuracy of 75%, 70%–74%, and 71%–74%, respectively. These values were not markedly different from those previously reported (7–13). However, our results show low positive predictive values of 27%–30% for both magnetic field strengths. Although sensitivity and specificity are considered inherent invariant test characteristics, predictive values depend not only on sensitivity and specificity but also on disease prevalence (30). This leads us to believe that the low positive predictive value of our results can be explained, at least in part, by the low prevalence of parametrial invasion in our study population.

As for vaginal invasion, reader 1 identified more true-positive cases than did reader 2. However, specificity was lower for reader 1 than for reader 2, and the area under the receiver operating characteristic curve was almost the same for the two readers. Moreover, interobserver agreement in the diagnosis of vaginal invasion was lower than that in the diagnosis of parametrial invasion and lymph node metastases. This indicates that the two readers had different thresholds for diagnosing vaginal invasion. In addition, intermodality agreement between 3.0- and 1.5-T imaging for diagnosis of vaginal invasion was also lower than that for parametrial invasion and lymph node metastases. These findings reflect difficulty in diagnosing vaginal invasion.

The quality of image homogeneity for 3.0-T imaging was inferior to that for 1.5-T imaging, in spite of the fact that we used a dielectric pad. Image inhomogeneity is the result of insufficient radiofrequency penetration and is usually severe in obese patients or those with massive ascites at presentation (14). Although our results show no significant difference between the imagers in terms of diagnostic performance, it may be better to use 1.5-T imagers rather than 3.0-T units to examine such patients whenever possible.

Magnetic susceptibility artifacts can theoretically be expected to double when moving from a 1.5-T imager to a 3.0-T unit (14,15). A previous study of 3.0-T imaging revealed no substantial susceptibility artifacts that deteriorated diagnostic performance in the preoperative evaluation of patients with endometrial carcinoma (20). Because the uterine cervix is closer to the rectum than the endometrium, we expected the

**Figure 4**

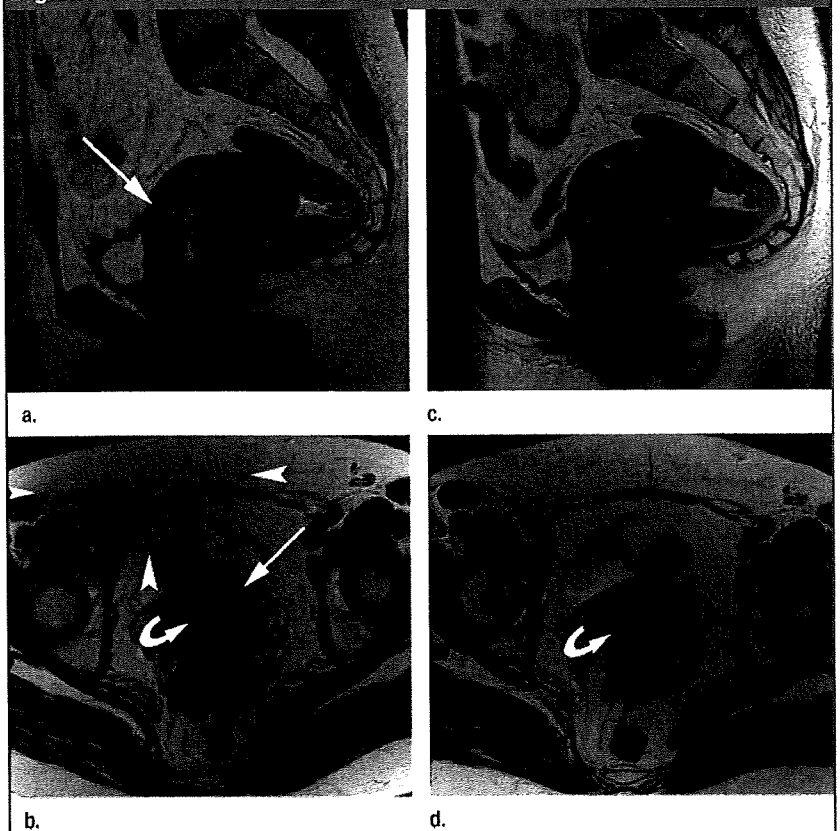


**Figure 4:** T2-weighted fast spin-echo MR images in a 43-year-old woman with cervical carcinoma (squamous cell carcinoma, keratinizing type, pT2b). Oblique 3.0-T images (6000/90; echo train length, 18) in the **(a)** parasagittal and **(b)** paraxial planes of the uterus clearly show the tumor (arrow). Oblique 1.5-T images (4000/90; echo train length, 12) in the **(c)** parasagittal and **(d)** paraxial planes of the uterus also show the tumor. Signal loss artifact due to radiofrequency inhomogeneity is seen on **b** (arrowheads). Oblique paraxial images (**b** and **d**) show disruption of the low-signal-intensity stromal ring (curved arrow); however, no protrusion into the parametrium is seen. It was difficult for either reader to confidently diagnose parametrial invasion on 3.0- or 1.5-T images.

susceptibility artifacts to be more substantial when we attempted to diagnose cervical carcinoma than when we tried to diagnose endometrial carcinoma. However, there were no significant differences in the degree of susceptibility artifacts between 3.0- and 1.5-T imaging in our series.

Some imaging parameters—specifically repetition time, echo train length, and receiver bandwidth—used for 3.0-T imaging differed from those used for 1.5-T imaging. Although optimal imaging parameters may differ between 3.0- and 1.5-T imaging, some radiologists use the same parameters for both examinations (16). The T1 relaxation times are longer for 3.0-T imaging than for 1.5-T imaging (31,32), reportedly by 42% for the uterine cervix (32). Thus, a longer repetition time would be needed to obtain T2-weighted 3.0-T images that were as good as those obtained with 1.5-T imaging; however, imaging times would also be longer if echo train length was not adjusted. If echo train length is increased to maintain practical imaging times, image blurring may become prominent. With these considerations, we used longer repetition time and echo train length for 3.0-T imaging than for 1.5-T imaging. We found that 3.0-T T2-weighted fast spin-echo images (6000/90; echo train length, 18) showed similar diagnostic accuracy for presurgical evaluation of patients with cervical carcinoma without a prominent increase in imaging time compared with 1.5-T T2-weighted fast spin-echo images (4000/90; echo train length, 12).

In our study, we assessed the accuracy of staging. However, for preoperative evaluation of radical trachelectomy, which is a fertility-preserving alternative to hysterectomy performed in patients with early-stage disease, tumor staging based on the International Federation of Gynecology and Obstetrics system would not be sufficient, and assessment of tumor extension proximal to the internal os would become crucial (33).

Our study had limitations. We compared only T2-weighted images, and we did not evaluate dynamic con-

**Table 2**

**Statistical Values for MR Assessment of Parametrial Invasion, Vaginal Invasion, and Lymph Node Metastases**

**A: Sensitivity, Specificity, and $A_z$**

| Reader | $A_z$ | Sensitivity (%) | Specificity (%) |
|---|---|---|---|
| 1 | | | |
| Parametrial invasion | | | |
| 3.0-T imaging | 0.82 | 75 (3/4) [33, 100] | 70 (19/27) [53, 88] |
| 1.5-T imaging | 0.85 | 75 (3/4) [33, 100] | 70 (19/27) [53, 88] |
| Vaginal invasion | | | |
| 3.0-T imaging | 0.62 | 67 (4/6) [29, 100] | 68 (17/25) [50, 86] |
| 1.5-T imaging | 0.67 | 67 (4/6) [29, 100] | 72 (18/25) [54, 90] |
| Lymph node metastases | | | |
| 3.0-T imaging | 0.72 | 57 (4/7) [20, 94] | 83 (20/24) [68, 98] |
| 1.5-T imaging | 0.78 | 57 (4/7) [20, 94] | 88 (21/24) [74, 100] |
| 2 | | | |
| Parametrial invasion | | | |
| 3.0-T imaging | 0.86 | 75 (3/4) [33, 100] | 74 (20/27) [58, 91] |
| 1.5-T imaging | 0.85 | 75 (3/4) [33, 100] | 70 (19/27) [53, 88] |
| Vaginal invasion | | | |
| 3.0-T imaging | 0.71 | 33 (2/6) [0, 71] | 84 (21/25) [70, 98] |
| 1.5-T imaging | 0.66 | 33 (2/6) [0, 71] | 92 (23/25) [81, 100] |
| Lymph node metastases | | | |
| 3.0-T imaging | 0.79 | 57 (4/7) [20, 94] | 88 (21/24) [74, 100] |
| 1.5-T imaging | 0.71 | 57 (4/7) [20, 94] | 88 (21/24) [74, 100] |

**B: Accuracy, PPV, and NPV**

| Reader | Accuracy (%) | PPV (%) | NPV (%) |
|---|---|---|---|
| 1 | | | |
| Parametrial invasion | | | |
| 3.0-T imaging | 71 (22/31) [55, 87] | 27 (3/11) [1, 54] | 95 (19/20) [85, 100] |
| 1.5-T imaging | 71 (22/31) [55, 87] | 27 (3/11) [1, 54] | 95 (19/20) [85, 100] |
| Vaginal invasion | | | |
| 3.0-T imaging | 68 (21/31) [51, 84] | 33 (4/12) [7, 60] | 89 (17/19) [76, 100] |
| 1.5-T imaging | 71 (22/31) [55, 87] | 36 (4/11) [8, 65] | 90 (18/20) [77, 100] |
| Lymph node metastases | | | |
| 3.0-T imaging | 77 (24/31) [63, 92] | 50 (4/8) [15, 85] | 87 (20/23) [73, 100] |
| 1.5-T imaging | 81 (25/31) [67, 95] | 57 (4/7) [20, 94] | 88 (21/24) [74, 100] |
| 2 | | | |
| Parametrial invasion | | | |
| 3.0-T imaging | 74 (23/31) [59, 90] | 30 (3/10) [2, 58] | 95 (20/21) [86, 100] |
| 1.5-T imaging | 71 (22/31) [55, 87] | 27 (3/11) [1, 54] | 95 (19/20) [85, 100] |
| Vaginal invasion | | | |
| 3.0-T imaging | 74 (23/31) [59, 90] | 33 (2/6) [0, 71] | 84 (21/25) [70, 98] |
| 1.5-T imaging | 81 (25/31) [67, 95] | 50 (2/4) [1, 99] | 85 (23/27) [72, 99] |
| Lymph node metastases | | | |
| 3.0-T imaging | 81 (25/31) [67, 95] | 57 (4/7) [20, 94] | 88 (21/24) [74, 100] |
| 1.5-T imaging | 81 (25/31) [67, 95] | 57 (4/7) [20, 94] | 88 (21/24) [74, 100] |

Note.—Data in parentheses are those used to calculate sensitivity, specificity, accuracy, and positive and negative predictive values. Data in brackets are 95% confidence intervals. There were no significant differences between 3.0- and 1.5-T imaging in terms of area under the receiver operating characteristic curve ($A_z$), sensitivity, and specificity values determined by each reader ($P > .5$ for all comparison pairs). NPV = negative predictive value, PPV = positive predictive value.

**Figure 5**

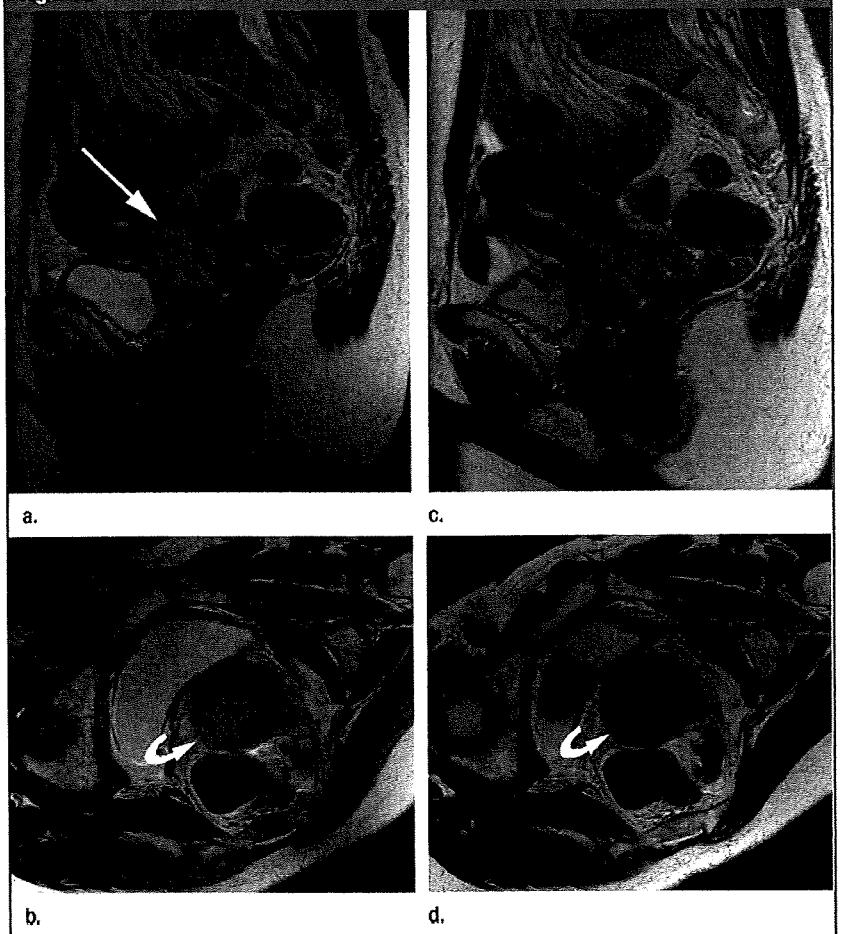


**Figure 5:** T2-weighted fast spin-echo MR images in a 51-year-old woman with cervical carcinoma (serous adenocarcinoma, pT2b). Oblique 3.0-T images (6000/90; echo train length, 18) in the **(a)** parasagittal and **(b)** paraxial planes of the uterus clearly show the tumor (straight arrow). Oblique 1.5-T images (4000/90; echo train length, 12) in the **(c)** parasagittal and **(d)** paraxial planes of the uterus also show the tumor. Oblique paraxial images (**b** and **d**) show disruption of the low-intensity stromal ring (curved arrow) and the tumor protruding into the right parametrium. Both readers confidently diagnosed parametrial invasion on both 3.0- and 1.5-T images.

**Table 3**

**κ Values for Interobserver and Intermodality Agreement**

| | Interobserver Agreement | | Intermodality Agreement | |
|---|---|---|---|---|
| Parameter | Reader 1 | Reader 2 | 3.0-T Imaging | 1.5-T Imaging |
| Parametrial invasion | 0.89 | 0.86 | 0.91 | 0.88 |
| Vaginal invasion | 0.76 | 0.65 | 0.77 | 0.74 |
| Lymph node metastases | 0.87 | 0.86 | 0.93 | 0.85 |

Note.—The κ values were calculated from the five-point scale scores assigned by the two readers for the presence of parametrial invasion, vaginal invasion, and lymph node metastases by using weighted κ statistics (quadratic weighting) to evaluate interobserver and intermodality agreement.

trast-enhanced MR images, even though some authors have reported that dynamic MR imaging was useful in the evaluation of cervical carcinoma (34). However, other studies have shown that dynamic MR imaging has limited value in the assessment of tumor extent (35,36) and that the role of contrast enhanced imaging is still a matter of debate (5). Furthermore, we thought our patients would be at greater risk if they received two injections of contrast material to compare the efficacy of 3.0-T dynamic MR imaging with that of 1.5-T imaging. Thus, we focused on T2-weighted imaging in this study; however, further study will be needed to evaluate the diagnostic capability of contrast-enhanced 3.0-T MR imaging.

We did not use special techniques—such as parallel imaging, flip angle refocusing, or higher-spatial-resolution techniques—for 3.0-T imaging. We potentially could have achieved better image quality if we used these techniques or if we used a more recently developed 3.0-T unit. This was another limitation of our study, especially because high-spatial-resolution 3.0-T imaging might have yielded more clinically relevant information (18).

Our study was also limited by the relatively small number of patients included ($n$ = 31) and the actual number of patients with local invasion. Larger sample sizes are needed to evaluate the diagnostic performance with greater precision. One patient did not undergo pelvic lymphadenectomy. This means that our results for the diagnosis of lymph node metastases may be somewhat inaccurate. However, it is unlikely that this was a substantial drawback because only one of 31 patients did not undergo pelvic lymphadenectomy.

Recall bias could be another limitation of our study because one of the two radiologists who reviewed images in terms of diagnostic performance analysis was involved in the clinical care of some of the patients. However, this was unlikely to be a substantial limitation because another radiologist who was not involved in the clinical care of these patients also reviewed the images, and κ analysis showed excellent or good interobserver agreement.

In conclusion, 3.0-T MR imaging had high diagnostic accuracy in the presurgical evaluation of patients with cervical carcinoma; however, this accuracy was not significantly superior to that of 1.5-T imaging. However, image inhomogeneity due to insufficient radiofrequency penetration was more significant at 3.0-T imaging than at 1.5-T imaging. Thus, it may be better to use 1.5-T MR imaging when evaluating certain patients, such as those who are obese or have massive ascites at presentation.

## References

1. American Cancer Society. Cancer facts and figures 2008. Atlanta, Ga: American Cancer Society, 2008.
2. Miller AB, Lindsay J, Hill GB. Mortality from cancer of the uterus in Canada and its relationship to screening for cancer of the cervix. Int J Cancer 1976;17(5):602–612.
3. Devesa SS, Young JL Jr, Brinton LA, Fraumeni JF Jr. Recent trends in cervix uteri cancer. Cancer 1989;64(10):2184–2190.
4. Benedet JL, Anderson GH, Matisic JP. A comprehensive program for cervical cancer detection and management. Am J Obstet Gynecol 1992;166(4):1254–1259.
5. Koyama T, Tamai K, Togashi K. Staging of carcinoma of the uterine cervix and endometrium. Eur Radiol 2007;17(8):2009–2019.
6. Van Nagell JR Jr, Roddick JW Jr, Lowin DM. The staging of cervical cancer: inevitable discrepancies between clinical staging and pathologic findinges. Am J Obstet Gynecol 1971;110(7):973–978.
7. Hricak H, Lacey CG, Sandles LG, Chang YC, Winkler ML, Stern JL. Invasive cervical carcinoma: comparison of MR imaging and surgical findings. Radiology 1988;166(3):623–631.
8. Togashi K, Nishimura K, Itoh K, et al. Uterine cervical cancer: assessment with high-field MR imaging. Radiology 1986;160(2):431–435.
9. Togashi K, Nishimura K, Sagoh T, et al. Carcinoma of the cervix: staging with MR imaging. Radiology 1989;171(1):245–251.
10. Kim SH, Choi BI, Lee HP, et al. Uterine cervical carcinoma: comparison of CT and MR findings. Radiology 1990;175(1):45–51.
11. Hricak H, Powell CB, Yu KK, et al. Invasive cervical carcinoma: role of MR imaging in pretreatment work-up—cost minimization and diagnostic efficacy analysis. Radiology 1996;198(2):403–409.
12. Bipat S, Glas AS, van der Velden J, Zwinderman AH, Bossuyt PM, Stoker J. Computed tomography and magnetic resonance imaging in staging of uterine cervical carcinoma: a systematic review. Gynecol Oncol 2003;91(1):59–66.
13. Hricak H, Gatsonis C, Chi DS, et al. Role of imaging in pretreatment evaluation of early invasive cervical cancer: results of the intergroup study American College of Radiology Imaging Network 6651-Gynecologic Oncology Group 183. J Clin Oncol 2005;23(36):9329–9337.
14. Merkle EM, Dale BM. Abdominal MRI at 3.0 T: the basics revisited. AJR Am J Roentgenol 2006;186(6):1524–1532.
15. Kuhl CK, Traber F, Schild HH. Whole-body high-field-strength (3.0-T) MR imaging in clinical practice. I. Technical considerations and clinical applications. Radiology 2008;246(3):675–696.
16. Morakkabati-Spitz N, Gieseke J, Kuhl C, et al. 3.0-T high-field magnetic resonance imaging of the female pelvis: preliminary experiences. Eur Radiol 2005;15(4):639–644.
17. Morakkabati-Spitz N, Schild HH, Kuhl CK, et al. Female pelvis: MR imaging at 3.0 T with sensitivity encoding and flip-angle sweep technique. Radiology 2006;241(2):538–545.
18. Morakkabati-Spitz N, Gieseke J, Kuhl C, et al. MRI of the pelvis at 3 T: very high spatial resolution with sensitivity encoding and flip-angle sweep technique in clinically acceptable scan time. Eur Radiol 2006;16(3):634–641.
19. Kataoka M, Kido A, Koyama T, et al. MRI of the female pelvis at 3T compared to 1.5T: evaluation on high-resolution T2-weighted and HASTE images. J Magn Reson Imaging 2007;25(3):527–534.
20. Torricelli P, Ferraresi S, Fiocchi F, et al. 3-T MRI in the preoperative evaluation of depth of myometrial infiltration in endometrial cancer. AJR Am J Roentgenol 2008;190(2):489–495.
21. Piver MS, Rutledge F, Smith JP. Five classes of extended hysterectomy for women with cervical cancer. Obstet Gynecol 1974;44(2):265–272.
22. Schmitt M, Feiweier T, Horger W, et al. Improved uniformity of RF-distribution in clinical whole body-imaging at 3T by means of dielectric pads [abstr]. In: Proceedings of the 12th Meeting of the International Society for Magnetic Resonance in Medicine. Berkeley, Calif: International Society for Magnetic Resonance in Medicine, 2004; 197.
23. Yang QX, Mao W, Wang J, et al. Manipulation of image intensity distribution at 7.0 T: passive RF shimming and focusing with dielectric materials. J Magn Reson Imaging 2006;24(1):197–202.
24. Landis JR, Koch GG. The measurement of observer agreement for categorical data. Biometrics 1977;33(1):159–174.
25. Gibbs GF, Huston J 3rd, Bernstein MA, Riederer SJ, Brown RD Jr. Improved image quality of intracranial aneurysms: 3.0-T versus 1.5-T time-of-flight MR angiography. AJNR Am J Neuroradiol 2004;25(1):84–87.
26. Kuhl CK, Textor J, Gieseke J, et al. Acute and subacute ischemic stroke at high-field-strength (3.0-T) diffusion-weighted MR imaging: intraindividual comparative study. Radiology 2005;234(2):509–516.
27. Norris DG. High field human imaging. J Magn Reson Imaging 2003;18(5):519–529.
28. Schick F. Whole-body MRI at high field: technical limits and clinical potential. Eur Radiol 2005;15(5):946–959.
29. Edelman RR, Salanitri G, Brand R, et al. Magnetic resonance imaging of the pancreas at 3.0 tesla: qualitative and quantitative comparison with 1.5 tesla. Invest Radiol 2006;41(2):175–180.
30. Halpern EF, Gazelle GS. Probability in radiology. Radiology 2003;226(1):12–15.
31. Bottomley PA, Foster TH, Argersinger RE, Pfeifer LM. A review of normal tissue hydrogen NMR relaxation times and relaxation mechanisms from 1–100 MHz: dependence on tissue type, NMR frequency, temperature, species, excision, and age. Med Phys 1984;11(4):425–448.
32. de Bazelaire CM, Duhamel GD, Rofsky NM, Alsop DC. MR imaging relaxation times of abdominal and pelvic tissues measured in vivo at 3.0 T: preliminary results. Radiology 2004;230(3):652–659.
33. Peppercorn PD, Jeyarajah AR, Woolas R, et al. Role of MR imaging in the selection of patients with early cervical carcinoma for fertility-preserving surgery: initial experience. Radiology 1999;212(2):395–399.
34. Yamashita Y, Takahashi M, Sawada T, Miyazaki K, Okamura H. Carcinoma of the cervix: dynamic MR imaging. Radiology 1992;182(3):643–648.
35. Fujiwara K, Yoden E, Asakawa T, et al. Negative MRI findings with invasive cervical biopsy may indicate stage IA cervical carcinoma. Gynecol Oncol 2000;79(3):451–456.
36. Scheidler J, Heuck AF, Steinborn M, Kimmig R, Reiser MF. Parametrial invasion in cervical carcinoma: evaluation of detection at MR imaging with fat suppression. Radiology 1998;206(1):125–129.

# Radiology 2009

## This is your reprint order form or pro forma invoice

**(Please keep a copy of this document for your records.)**

Reprint order forms and purchase orders or prepayments must be received 72 hours after receipt of form either by mail or by fax at 410-820-9765. It is the policy of Cadmus Reprints to issue one invoice per order. **Please print clearly.**

Author Name _____

Title of Article _____

Issue of Journal _____ Reprint # _____ Publication Date _____

Number of Pages _____ KB # _____ Symbol Radiology

Color in Article? Yes / No (Please Circle)

**Please include the journal name and reprint number or manuscript number on your purchase order or other correspondence.**

### Order and Shipping Information

**Reprint Costs** (Please see page 2 of 2 for reprint costs/fees.)

_____ Number of reprints ordered $_____

_____ Number of color reprints ordered $_____

_____ Number of covers ordered $_____

**Subtotal** $_____

Taxes $_____

*(Add appropriate sales tax for Virginia, Maryland, Pennsylvania, and the District of Columbia or Canadian GST to the reprints if your order is to be shipped to these locations.)*

First address included, add $32 for each additional shipping address $_____

**TOTAL** $_____

**Shipping Address** (cannot ship to a P.O. Box) Please Print Clearly

Name _____

Institution _____

Street _____

City _____ State _____ Zip _____

Country _____

Quantity _____ Fax _____

Phone: Day _____ Evening _____

E-mail Address _____

**Additional Shipping Address*** (cannot ship to a P.O. Box)

Name _____

Institution _____

Street _____

City _____ State _____ Zip _____

Country _____

Quantity _____ Fax _____

Phone: Day _____ Evening _____

E-mail Address _____

** Add $32 for each additional shipping address*

### Payment and Credit Card Details

**Enclosed**: Personal Check _____

Credit Card Payment Details _____

Checks must be paid in U.S. dollars and drawn on a U.S. Bank.

Credit Card: __ VISA __ Am. Exp. __ MasterCard

Card Number _____

Expiration Date _____

Signature: _____

Please send your order form and prepayment made payable to:

**Cadmus Reprints**
**P.O. Box 751903**
**Charlotte, NC 28275-1903**

***Note: Do not send express packages to this location, PO Box.***

*FEIN #:541274108*

### Invoice or Credit Card Information

**Invoice Address** **Please Print Clearly**

**Please complete Invoice address as it appears on credit card statement**

Name _____

Institution _____

Department _____

Street _____

City _____ State _____ Zip _____

Country _____

Phone _____ Fax _____

E-mail Address _____

**Cadmus will process credit cards and *Cadmus Journal Services* will appear on the credit card statement.**

***If you don't mail your order form, you may fax it to 410-820-9765 with your credit card information.***

Signature _____ Date _____

Signature is required. By signing this form, the author agrees to accept the responsibility for the payment of reprints and/or all charges described in this document.

RB-1/01/09

**Page 1 of 2**

# Radiology 2009

## Black and White Reprint Prices

| Domestic (USA only) | | | | | | |
|---|---|---|---|---|---|---|
| # of Pages | 50 | 100 | 200 | 300 | 400 | 500 |
| 1-4 | $239 | $260 | $285 | $303 | $323 | $340 |
| 5-8 | $379 | $420 | $455 | $491 | $534 | $572 |
| 9-12 | $507 | $560 | $651 | $684 | $748 | $814 |
| 13-16 | $627 | $698 | $784 | $868 | $954 | $1,038 |
| 17-20 | $755 | $845 | $947 | $1,064 | $1,166 | $1,272 |
| 21-24 | $878 | $985 | $1,115 | $1,250 | $1,377 | $1,518 |
| 25-28 | $1,003 | $1,136 | $1,294 | $1,446 | $1,607 | $1,757 |
| 29-32 | $1,128 | $1,281 | $1,459 | $1,632 | $1,819 | $2,002 |
| Covers | $149 | $164 | $219 | $275 | $335 | $393 |

| International (includes Canada and Mexico) | | | | | | |
|---|---|---|---|---|---|---|
| # of Pages | 50 | 100 | 200 | 300 | 400 | 500 |
| 1-4 | $299 | $314 | $367 | $429 | $484 | $546 |
| 5-8 | $470 | $502 | $616 | $722 | $838 | $949 |
| 9-12 | $637 | $687 | $852 | $1,031 | $1,190 | $1,369 |
| 13-16 | $794 | $861 | $1,088 | $1,313 | $1,540 | $1,765 |
| 17-20 | $963 | $1,051 | $1,324 | $1,619 | $1,892 | $2,168 |
| 21-24 | $1,114 | $1,222 | $1,560 | $1,906 | $2,244 | $2,588 |
| 25-28 | $1,287 | $1,412 | $1,801 | $2,198 | $2,607 | $2,998 |
| 29-32 | $1,441 | $1,586 | $2,045 | $2,499 | $2,959 | $3,418 |
| Covers | $211 | $224 | $324 | $444 | $558 | $672 |

Minimum order is 50 copies. For orders larger than 500 copies, please consult Cadmus Reprints at 800-407-9190.

## Reprint Cover

Cover prices are listed above. The cover will include the publication title, article title, and author name in black.

## Shipping

Shipping costs are included in the reprint prices. Domestic orders are shipped via FedEx Ground service. Foreign orders are shipped via a proof of delivery air service.

## Multiple Shipments

Orders can be shipped to more than one location. Please be aware that it will cost $32 for each additional location.

## Delivery

Your order will be shipped within 2 weeks of the journal print date. Allow extra time for delivery.

## Color Reprint Prices

| Domestic (USA only) | | | | | | |
|---|---|---|---|---|---|---|
| # of Pages | 50 | 100 | 200 | 300 | 400 | 500 |
| 1-4 | $247 | $267 | $385 | $515 | $650 | $780 |
| 5-8 | $297 | $435 | $655 | $923 | $1194 | $1467 |
| 9-12 | $445 | $563 | $926 | $1,339 | $1,748 | $2,162 |
| 13-16 | $587 | $710 | $1,201 | $1,748 | $2,297 | $2,843 |
| 17-20 | $738 | $858 | $1,474 | $2,167 | $2,846 | $3,532 |
| 21-24 | $888 | $1,005 | $1,750 | $2,575 | $3,400 | $4,230 |
| 25-28 | $1,035 | $1,164 | $2,034 | $2,986 | $3,957 | $4,912 |
| 29-32 | $1,186 | $1,311 | $2,302 | $3,402 | $4,509 | $5,612 |
| Covers | $149 | $164 | $219 | $275 | $335 | $393 |

| International (includes Canada and Mexico)) | | | | | | |
|---|---|---|---|---|---|---|
| # of Pages | 50 | 100 | 200 | 300 | 400 | 500 |
| 1-4 | $306 | $321 | $467 | $642 | $811 | $986 |
| 5-8 | $387 | $517 | $816 | $1,154 | $1,498 | $1,844 |
| 9-12 | $574 | $689 | $1,157 | $1,686 | $2,190 | $2,717 |
| 13-16 | $754 | $874 | $1,506 | $2,193 | $2,883 | $3,570 |
| 17-20 | $710 | $1,063 | $1,852 | $2,722 | $3,572 | $4,428 |
| 21-24 | $1,124 | $1,242 | $2,195 | $3,231 | $4,267 | $5,300 |
| 25-28 | $1,320 | $1,440 | $2,541 | $3,738 | $4,957 | $6,153 |
| 29-32 | $1,498 | $1,616 | $2,888 | $4,269 | $5,649 | $7028 |
| Covers | $211 | $224 | $324 | $444 | $558 | $672 |

## Tax Due

Residents of Virginia, Maryland, Pennsylvania, and the District of Columbia are required to add the appropriate sales tax to each reprint order. For orders shipped to Canada, please add 7% Canadian GST unless exemption is claimed.

## Ordering

Reprint order forms and purchase order or prepayment is required to process your order. Please reference journal name and reprint number or manuscript number on any correspondence. You may use the reverse side of this form as a proforma invoice. Please return your order form and prepayment to:

**Cadmus Reprints**
P.O. Box 751903
Charlotte, NC 28275-1903

***Note: Do not send express packages to this location, PO Box.***
*FEIN #:541274108*

**Please direct all inquiries to:**

*Rose A. Baynard*
800-407-9190 (toll free number)
410-819-3966 (direct number)
410-820-9765 (FAX number)
baynardr@cadmus.com (e-mail)

**Reprint Order Forms and purchase order or prepayments must be received 72 hours after receipt of form.**

Gynecologic Oncology 115 (2009) 482–487

Contents lists available at ScienceDirect

Gynecologic Oncology

journal homepage: www.elsevier.com/locate/ygyno

# Postoperative concurrent nedaplatin-based chemoradiotherapy improves survival in early-stage cervical cancer patients with adverse risk factors

Seiji Mabuchi [a,*], Ken-ichirou Morishige [a], Fumiaki Isohashi [b], Yasuo Yoshioka [b], Takashi Takeda [a], Toshiya Yamamoto [a], Kiyoshi Yoshino [a], Takayuki Enomoto [a], Takehiro Inoue [b], Tadashi Kimura [a]

[a] Department of Obstetrics and Gynecology, Osaka University Graduate School of Medicine, 2-2 Yamadaoka, Suita, Osaka 565-0871, Japan
[b] Department of Radiation Oncology, Osaka University Graduate School of Medicine, 2-2 Yamadaoka, Suita, Osaka 565-0871, Japan

ARTICLE INFO

*Article history:*
Received 21 May 2009
Available online 23 September 2009

*Keywords:*
Postoperative chemoradiotherapy
Early-stage cervical cancer
Nedaplatin
Survival
Radical hysterectomy

ABSTRACT

*Objectives.* The aim of this study was to evaluate the efficacy of postoperative nedaplatin-based concurrent chemoradiotherapy (CCRT) in patients with FIGO stage IA2–IIB cervical cancer with adverse risk factors.

*Methods.* We retrospectively reviewed the medical records of 183 patients with early-stage cervical cancer who had undergone radical surgery between April 1997 and March 2006. Of these, 68 patients displayed high-risk prognostic factors such as positive pelvic lymph nodes, parametrial involvement, or a positive surgical margin. Fifty-seven patients demonstrated intermediate-risk prognostic factors including deep stromal invasion, capillary lymphatic space involvement, or large tumor diameter. These patients were treated postoperatively with CCRT or radiotherapy alone (RT). Fifty-eight patients showed no risk factors and, therefore, received no adjuvant therapy after surgery. The 3-year recurrence rate, progression free survival (PFS), and overall survival (OS) were compared between the treatment groups.

*Results.* CCRT was significantly superior to RT alone with regard to recurrence rate, PFS, and OS in patients that displayed high-risk and intermediate-risk prognostic factors. The frequencies of acute grade 3–4 toxicities were significantly higher in patients treated with CCRT than in those treated with RT alone. However, no statistically significant difference was observed with regard to severe late toxicities.

*Conclusions.* Postoperative nedaplatin-based CCRT was safely performed and improved the prognosis of FIGO stage IA2–IIB cervical cancer patients displaying high-risk or intermediate-risk prognostic factors. This treatment can be considered as an alternative to cisplatin-based chemoradiotherapy in this patient population.


## Introduction

Early-stage cervical cancer has traditionally been treated by either radical hysterectomy or primary radiotherapy with similar survival outcomes. According to previous reports, the 5-year survival rate of patients with FIGO stage IB–IIA cervical cancer treated with radical surgery has been reported to be 83–91%, which is comparable to the 74–91% reported for those treated with radiotherapy alone [1-3]. In Japan, patients with stage IA2–IIB cervical cancer are usually treated with radical surgery [4,5].

Several risk factors have been identified that compromise the treatment outcome in patients with early-stage cervical cancer who were primarily treated with radical surgery [6-8]. Generally, patients with risk factors such as positive pelvic nodes, parametrial invasion, or a positive vaginal margin are regarded as "high-risk" for recurrence [6]. Moreover, patients with a tumor confined to the cervix that display risk factors such as large tumor size, lymphovascular space invasion, and deep stromal invasion are considered to be at "intermediate-risk" of recurrence [7, 8]. Postoperative RT is usually recommended for patients that display these risk factors.

A previous Gynecologic Oncology Group Phase III study (GOG 92) evaluated the role of adjuvant RT in patients that showed "intermediate-risk" prognostic factors, i.e., those with at least two of the following risk factors after radical hysterectomy: >1/3 stromal invasion, lymphovascular space involvement, or large tumor diameter. Although overall survival was not significantly prolonged by the addition of adjuvant RT, this study demonstrated that adjuvant RT significantly reduced the risk of recurrence and prolonged progression free survival in these women [9,10].

In early-stage cervical cancer patients with high-risk prognostic factors, a prospective randomized clinical trial (GOG 109/SWOG 87-97) addressed the role of adjuvant concurrent chemoradiotherapy (CCRT) after radical hysterectomy and pelvic lymphadenectomy [11]. The

*Abbreviations:* CT, computed tomography; MRI, magnetic resonance imaging; OS, overall survival; PFS, progression free interval; ICBT, intracavitary brachytherapy; EBRT, external beam radiotherapy; RT, radiotherapy; CCRT, concurrent chemoradiotherapy.

* Corresponding author. Fax: +81 6 6879 3359.
*E-mail address:* smabuchi@gyne.med.osaka-u.ac.jp (S. Mabuchi).

0090-8258/$ – see front matter © 2009 Elsevier Inc. All rights reserved.
doi:10.1016/j.ygyno.2009.09.002

study demonstrated that the addition of concurrent cisplatin-based chemotherapy to postoperative RT improved survival in patients with positive pelvic LN and/or a positive resection margin and/or parametrial involvement.

Concurrent chemoradiotherapy, usually with 40 mg/m$^2$ of weekly cisplatin, is now accepted as a standard first line treatment for cervical cancer [12,13]. However, in a previous Japanese phase I study, which determined the recommended dose of weekly cisplatin in the setting of CCRT after radical hysterectomy, dose-limiting toxicity (DLT) was observed at 40 mg/m$^2$, indicating that a weekly dose of 40 mg/m$^2$ of cisplatin may be too high for Japanese patients with cervical cancer [14]. Therefore, the use of an agent that shows less toxicity as a radiosensitizer may be beneficial for Japanese patients with cervical cancer.

Nedaplatin (*cis*-diammine-glycoplatinum), a derivative of cisplatin, was developed by Shionogi Pharmaceutical Company in Japan with the aim of ensuring reduced renal and gastrointestinal toxicity compared to cisplatin but similar effectiveness.

In a preclinical evaluation of cervical cancer, nedaplatin demonstrated significant anti-tumor activity similar to that of cisplatin [15,16]. Its lower incidence of nephrotoxicity in comparison to cisplatin has been demonstrated to be associated with a difference in the kidney distribution of these drugs. When the two agents were administered at the same dose, the concentration of nedaplatin in the rat kidney was approximately 40% of that of cisplatin, leading to lower nephrotoxicity [17,18].

Clinically, previous phase II studies conducted in Japan suggested that nedaplatin has a particularly favorable clinical efficacy on squamous cell carcinoma of the head and neck, esophagus, or uterine cervix [19,20]. In a phase II clinical trial, nedaplatin demonstrated a response rate of 46% in patients with recurrent cervical cancer, which was slightly superior to that obtained with cisplatin (39%) [21]. Moreover, since nedaplatin does not require hydration, the treatment is manageable in an outpatient setting. On the basis of these advantages, nedaplatin has been used clinically in Japan as an alternative to cisplatin for patients with recurrent cervical cancer [22].

The radio-sensitizing properties of nedaplatin have been demonstrated in several preclinical studies [23,24]. However, clinical experience with the use of this agent in the setting of CCRT in patients with cervical cancer is limited. The use of concurrent weekly nedaplatin in patients with invasive cervical cancer in the setting of primary radiotherapy was investigated in two phase I [14,25] and two phase II studies [26,27]; however, in the setting of adjuvant radiotherapy, nedaplatin-based CCRT has been evaluated only in one phase I study [28]. Thus, questions remain unanswered whether postoperative nedaplatin-based CCRT is superior to RT alone in patients with early-stage cervical cancer with intermediate-risk or high-risk prognostic factors. To answer this question, in the current study, we retrospectively evaluated the effectiveness of nedaplatin-based CCRT in Japanese patients with FIGO stage IA2–IIB cervical cancer after radical hysterectomy and pelvic lymphadenectomy.

## Materials and methods

### *Patients*

Permission to proceed with data acquisition and analysis was obtained from Osaka University Hospital's institutional review board. A list of patients who had undergone radical hysterectomy (type III) and pelvic lymphadenectomy for FIGO stage IA2–IIB cervical cancer at Osaka University Hospital from April 1997 to March 2006 was generated from our institutional tumor registry. Then, through a chart review, patients who required postoperative radiotherapy with or without nedaplatin-based concurrent chemotherapy because of the criteria outlined below were identified, and their clinical data were retrospectively reviewed. Patients were treated by postoperative radiotherapy when their pathological report displayed any one of the following "high-risk" prognostic factors: pelvic lymph node metastasis, positive parametrial involvement, or a positive surgical margin or one of the following "intermediate-risk" prognostic factors: deep stromal invasion, lymphovascular space invasion, or large tumor size (over 4 cm).

Based on the U.S. National Cancer Institute (NCI) alert in 1999 [13], we have started a clinical practice of nedaplatin-based adjuvant CCRT for patients with cervical cancer after radical surgery. Basically, nedaplatin-based adjuvant CCRT was indicated in all patients with intermediate-risk or high-risk prognostic factors below the age of 75 years old. However, patients who refused the use of concurrent chemotherapy and patients who had suffered from cervical cancer before the introduction of CCRT were treated with RT alone.

A group of patients with early-stage cervical cancer without any of the above mentioned adverse risk factors and who therefore did not receive postoperative adjuvant therapy were also identified through the chart review and served as the control (low-risk group).

The preoperative staging was performed according to the International Federation of Gynecology and Obstetrics staging criteria by a gynecological oncologist without general anesthesia.

### *Radiotherapy*

Postoperative radiotherapy was performed within 3 weeks of radical surgery. Pelvic radiotherapy was delivered using a 10 megavolt (MV) X-ray from a linear accelerator with the anteroposterior parallel opposing technique. The superior margin of the external radiation field was placed on the upper border of the fifth lumber vertebra, and the inferior margins were the inferior border of the obturator foramen. Laterally, the field extended 2 cm beyond the lateral margin of the bony pelvic wall. We used multi-leaf collimators to block the upper and lower corners of the radiation field. External irradiation was delivered to the whole pelvis at 2 Gy per fraction for 5 fractions per week, for a total of 25 fractions (50 Gy). Seven patients in the high-risk group that displayed vaginal invasion close to the surgical margin also received intracavitary radiotherapy (ICRT) of 30 Gy in five fractions at 5 mm below the vaginal mucosa after external beam radiotherapy (EBRT).

### *Chemotherapy*

Nedaplatin was given intravenously on a weekly basis during the course of EBRT for 5 weeks. The median number of cycles per patient was five (range: 2–5), and the median dose of nedaplatin was 40 mg/m$^2$ (range: 10–45). The first cycle of nedaplatin was initiated on the first day of radiotherapy treatment. The drug was given in a 1-h infusion. Renal function and blood counts were assessed before each cycle. Nedaplatin administration was suspended when the patient's granulocyte count was less than 1500/μl or their platelet count was less than 100,000/μl. Nedaplatin administration was also suspended if the patient could not tolerate the acute gastrointestinal toxicity induced during the course of treatment. In the weeks in which the patient did not receive chemotherapy, radiation was continued as long as their granulocyte count was higher than 1000/μl and their platelet count was higher than 50,000/μl.

### *Toxicity*

Clinical data regarding treatment-related complications were also collected. Complications that occurred within 90 days of the start of primary treatment were considered to be acute complications, and those that occurred more than 90 days after the start of treatment were considered as late complications. The severity of acute complications was classified according to the NCI Common

**Table 1**
Patients enrolled in this study.

| | | Low risk | Intermediate risk | High risk |
|---|---|---|---|---|
| Number of patients | | 58 | 57 | 68 |
| Age (mean) | | 42 | 49.7 | 50.7 |
| Clinical stage | IA2 | 9 | 0 | 0 |
| | IB | 49 | 43 | 19 |
| | IIA | 0 | 14 | 11 |
| | IIB | 0 | 0 | 38 |
| Histology | Squamous cell | 31 | 17 | 46 |
| | Adenocarcinoma | 26 | 37 | 21 |
| | Adenosquamous | 0 | 3 | 1 |
| | Others | 1 | 0 | 0 |

Terminology Criteria for Adverse Events, Version 2.0. Late complications were graded according to the Radiation Therapy Oncology Group (RTOG) Late Radiation Morbidity Scoring Scheme [29].

*Follow-up*

Patients were followed regularly and observed for acute and late toxicities by both gynecological oncologists and radiation oncologists. During the treatment, the patients were evaluated weekly by pelvic examination and complete blood counts. For patients treated with chemoradiation, renal and liver function tests were also performed weekly. After treatment completion, the patients were followed in an outpatient clinic every month in the first year, every 2 months in the second year, every 3 months in the third year, every 6 months in the fourth to fifth year, and annually thereafter until 10 years after treatment. Standard clinical surveillance consisted of a clinical history, physical examinations including abdominal, pelvic bimanual, and speculum examinations, and a pap smear from the vaginal vault. Chest X-ray and CT-scans were performed every 6 months in the first to third years and annually in the fourth and fifth years. When clinically indicated, imaging studies including abdominal or vaginal ultrasounds or MRI were performed. Patients who had bloody stools or hematuria underwent endoscopy to identify the site of the bleeding. Pelvic failure was defined as disease persisting or recurring in the pelvis, including central or parametrial failure. Distant failure was defined as disease occurring outside the pelvis, including the paraaortic lymph nodes. When local recurrence was suspected after pelvic examination or smears, a biopsy was taken for confirmation whenever possible. The median duration of follow-up was 36 months (range: 20–80 months).

**Table 2**
Patient characteristics (intermediate-risk patients).

| | | RT-group | CCRT-group | *P*-value |
|---|---|---|---|---|
| Number of patients | | 35 | 22 | |
| Age (mean) | | 49.8 | 49.6 | NS |
| Clinical stage | IA2 | 0 | 0 | NS |
| | IB | 25 | 18 | |
| | IIA | 10 | 4 | |
| | IIB | 0 | 0 | |
| Histology | Squamous cell | 27 | 13 | 0.04 |
| | Adenocarcinoma | 5 | 0 | |
| | Adenosquamous | 3 | 9 | |
| | Others | 0 | 0 | |
| Lymphovascular space involvement | Yes | 24 | 18 | NS |
| | No | 11 | 4 | |
| Stromal invasion | Less than one-half | 24 | 4 | 0 0003 |
| | More than one-half | 11 | 14 | |
| Tumor diameter | Mean (mm) | 29.4 | 26.5 | NS |
| Pretreatment hemoglobin level | Mean (mg/dl) | 12 | 12 | NS |
| Duration of radiotherapy | Days | 37 | 37 | NS |

*Statistical analysis*

The differences between the groups with respect to stage, histology, and risk factors such as node status, parametrial involvement, surgical margin status, deep stromal invasion, and lymphovascular space invasion were assessed using Fisher's exact test. Age, maximum tumor diameter, and the pretreatment hemoglobin level were compared using Welch's t-test. Treatment related toxicities were compared using Fisher's exact test. The survival analysis was based on the Kaplan–Meier method and compared by the log-rank test. PFS was defined as the time from the primary diagnosis to the detection of recurrence. OS was defined as the time from the primary diagnosis to death or the latest observation. *P*-values of $<0.05$ were considered statistically significant.

## Results

*Patient characteristics*

As shown in Table 1, among a total of 183 patients enrolled in the study, 68 patients displayed high-risk prognostic factors such as positive pelvic lymph nodes, parametrial involvement, or a positive surgical margin. Fifty-seven patients showed intermediate-risk prognostic factors such as deep stromal invasion, capillary lymphatic space involvement, or large tumor diameter. These patients were postoperatively treated with CCRT or RT alone. Fifty-eight patients displayed no risk factors and, therefore, received no adjuvant therapy after surgery.

Among the 57 patients that demonstrated intermediate-risk prognostic factors, 22 were treated with adjuvant CCRT, and 35 were treated with RT alone (Table 2). The characteristics of the patients in the RT-group were similar to those in the CCRT-group. When compared, there was no statistical difference in terms of age; clinical stage; or risk factors such as stromal invasion, lymphovascular involvement, tumor diameter, pretreatment hemoglobin, and the duration of radiotherapy. However, a significantly increased proportion of patients with adenocarcinoma histology or deep stromal invasion was observed in the CCRT-group.

As shown in Table 3, of the 68 patients that displayed high-risk prognostic risk factors, 34 received adjuvant CCRT, and 34 received adjuvant RT. When compared, there was no statistical difference in terms of age, clinical stage, histologic distribution, pelvic node status, tumor diameter, pretreatment hemoglobin, or the duration of radiotherapy. However, a significantly increased number of patients

**Table 3**
Patient characteristics (high-risk patients).

| | | RT-group | CCRT-group | *P*-value |
|---|---|---|---|---|
| Number of patients | | 34 | 34 | |
| Age (mean) | | 51.3 | 50.1 | NS |
| Clinical stage | IA2 | 0 | 0 | NS |
| | IB | 7 | 12 | |
| | IIA | 9 | 2 | |
| | IIB | 18 | 20 | NS |
| Histology | Squamous cell | 21 | 25 | |
| | Adenocarcinoma | 13 | 8 | |
| | Adenosquamous | 0 | 1 | |
| | Others | 0 | 0 | |
| Positive pelvic node | Yes | 23 | 22 | NS |
| | No | 11 | 12 | |
| Parametrial involvement | Yes | 18 | 20 | NS |
| | No | 16 | 14 | |
| Positive margins | Yes | 7 | 0 | 0.01 |
| | No | 0 | 0 | |
| Tumor diameter | Mean (mm) | 41.2 | 43 | NS |
| Pretreatment hemoglobin level | Mean (mg/dl) | 11.4 | 11.8 | NS |
| Duration of radiotherapy | Days | 38 | 38 | NS |

**Table 4**
Treatment outcome.

| Intermediate-risk patients | | RT-group ($n=35$) | CCRT-group ($n=22$) | *P*-value |
|---|---|---|---|---|
| Patients with recurrence (%) | | 12 (34.3) | 1 (4.5) | 0.01 |
| | Local | 7 | 0 | |
| | Local + distant | 3 | 1 | |
| | Distant | 2 | 0 | |
| PFS (months) | Mean | 29 | 36 | 0.0026 |
| OS (months) | Mean | 32.5 | 36 | 0.043 |
| **High-risk patients** | | **RT-group ($n=34$)** | **CCRT-group ($n=34$)** | ***P*-value** |
| Patients with recurrence (%) | | 16 (47.0) | 9 (26.5) | 0.1306 |
| | Local | 6 | 2 | |
| | Local + distant | 6 | 7 | |
| | Distant | 4 | 0 | |
| PFS (months) | Mean | 22.6 | 29.5 | 0.0812 |
| OS (months) | Mean | 29.7 | 34.2 | 0.0364 |

with vaginal invasion close to the surgical margin were observed in the RT-group.

*Treatment outcome*

In patients without any adverse risk prognostic factors (low-risk patients), no recurrence was observed within 3 years.

In the intermediate-risk group, as shown in Table 4, treatment failure was observed in 1 patient (4.5%) in the CCRT-group and 12 patients (34.2%) in the RT-group. The addition of concurrent nedaplatin-based chemotherapy resulted in significantly fewer local and distant relapses. The 3-year overall survival rate was 100% in the CCRT-group and 82.9% in the RT-group. When the CCRT-group was compared with the RT-group, as shown in Figs. 1A and B and Table 4, CCRT was significantly superior in terms of recurrence rate ($p=0.01$), PFS (log-rank; $p=0.0026$), and OS (log-rank; $p=0.0435$). When the intermediate-risk group was compared with the low-risk group, although significant differences in PFS and OS were observed in patients treated with RT alone, there were no significant differences in PFS or OS in the patients treated with CCRT (Fig. 2).

As shown in Table 4, in the patients that displayed high-risk prognostic factors, treatment failure was observed in 9 patients (26.5%) in the CCRT-group and 16 patients (47.1%) in the RT-group. The addition of concurrent nedaplatin-based chemotherapy also resulted in fewer local and distant relapses in this patient population. The 3-year overall survival rate was 88.2% in the CCRT-group and 67.6% in the RT-group. When the CCRT-group was compared with the RT-group, as shown in Figs. 1C and D and Table 4, CCRT was significantly superior in terms of OS (log-rank; $p=0.0364$). The difference in PFS did not reach statistical significance (log-rank; $p=0.0812$). When the high-risk group was compared with the low-risk group, significant differences in PFS and OS were observed both in the patients treated with RT alone and those treated with CCRT (Fig. 2).

*Adverse effects*

Generally, nedaplatin-based CCRT was well tolerated. There were no treatment-related deaths. Among a total of 56 patients treated with CCRT, grade 3 or 4 acute toxicities were observed in 36 patients (64.3%).

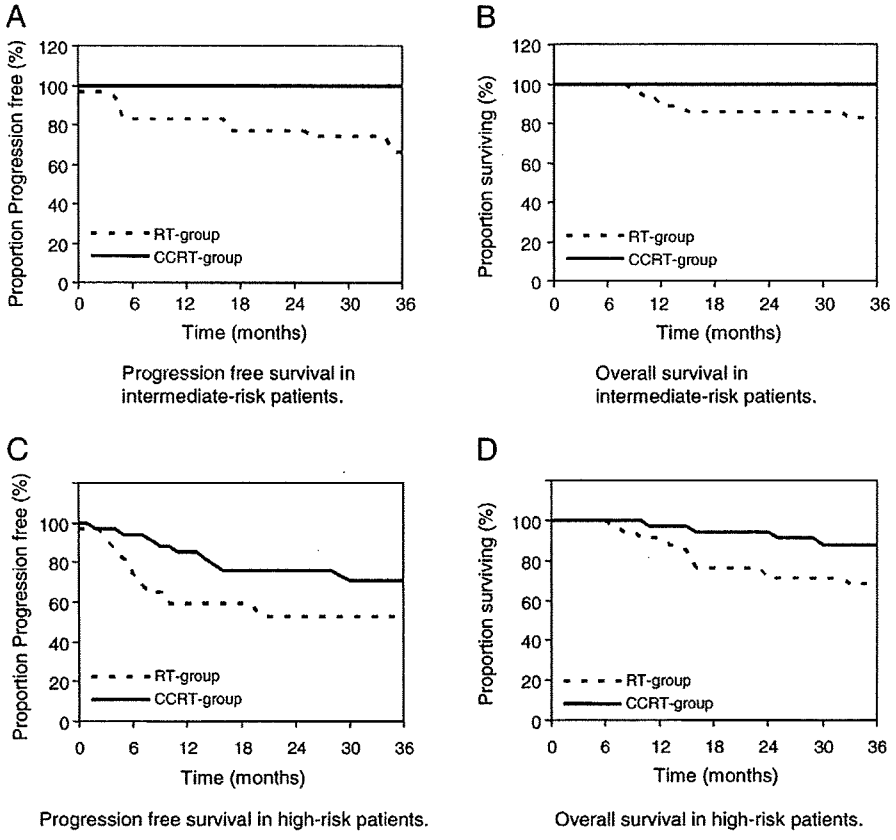


**Fig. 1.** (A) Progression free survival in intermediate-risk patients. The progression free survival rate was significantly higher among the patients in the CCRT-group ($p=0.0026$). (B) Overall survival in intermediate-risk patients. The overall survival rate was significantly higher among the patients in the CCRT-group ($p=0.043$). (C) Progression free survival in high-risk patients. The progression free survival rate was higher among the patients in the CCRT-group, but the difference was not statistically significant ($p=0.081$). (D) Overall survival in high-risk patients. The overall survival rate was significantly higher among the patients in the CCRT-group ($p=0.0364$).

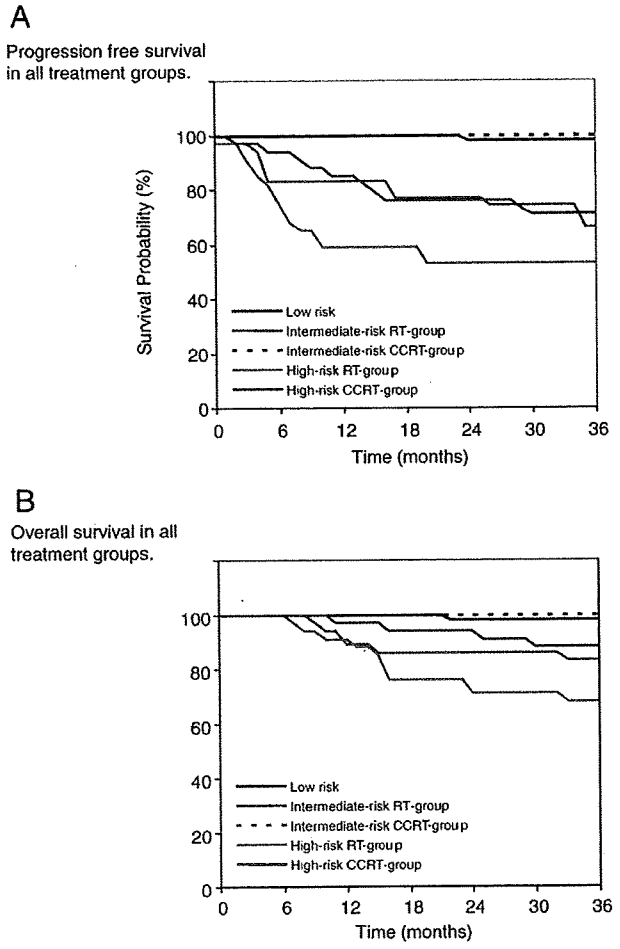


**Fig. 2.** (A) Progression free survival in all treatment groups. The progression free survival rate in the low-risk patients was equivalent to that in the intermediate-risk patients treated with CCRT ($p=0.5380$), but was significantly higher than that in the intermediate-risk patients treated with RT alone ($p<0.0001$). The progression free survival rate in the low-risk patients was significantly higher than that in the high-risk patients treated with RT alone ($p<0.0001$) or CCRT ($p<0.0001$). The progression free survival rate in the intermediate-risk patients treated with RT alone was equivalent to that in the high-risk patients treated with CCRT ($p=0.6729$). (B) Overall survival in all treatment groups. The overall survival rate in the low-risk patients was equivalent to that in the intermediate-risk patients treated with CCRT ($p=0.5380$), but significantly higher than that in the intermediate-risk patients treated with RT alone ($p=0.0058$). The overall survival rate in the low-risk patients was significantly higher than that in the high-risk patients treated with RT alone ($p<0.0001$) or CCRT ($p=0.0403$). The overall survival rate in the intermediate-risk patients treated with RT alone was similar to that in the high-risk patients treated with CCRT ($p=0.5003$).

Of these, 30 patients had neutropenia alone, and 3 had both neutropenia and thrombocytopenia. Three patients developed non-hematologic toxicities (bowel obstruction in one patient, diarrhea in one patient, and radiation dermatitis in one patient). Among a total of 69 patients treated with RT alone, grade 3 or 4 acute toxicities were observed in 8 patients (11.6%). Of these, four patients had neutropenia alone, and one had both neutropenia and thrombocytopenia. Three patients developed non-hematologic toxicities (bowel obstruction in one patient and diarrhea in two patients). All cases were successfully managed with conservative treatment. When compared, the frequencies of acute grade 3–4 toxicities were significantly higher in the patients treated with CCRT than in those treated with RT alone ($p<0.001$).

Grade 3–4 severe late toxicity was observed in one patient who received RT alone. This woman developed a vesicovaginal fistula 4 months after the completion of RT. No grade 3–4 late toxicity was observed in the patients treated with CCRT.

## Discussion

Based on the consistent results of five randomized controlled trials, CCRT, usually involving weekly cisplatin 40 mg/m$^2$ for 6 weeks in combination with RT, has become the standard treatment for locally advanced cervical cancer [11,30-33].

In the setting of adjuvant radiotherapy, only one sufficiently powered prospective randomized trial (GOG 109/SWOG 87-97) has examined the use of concurrent chemotherapy with RT after radical hysterectomy and lymphadenectomy [11]. In this trial, progression free survival (PFS) and overall survival (OS) were significantly improved by the addition of concurrent chemotherapy to external beam RT in patients that displayed high-risk factors such as positive pelvic lymph nodes, parametrial invasion, or a positive surgical margin.

In patients that showed intermediate-risk prognostic factors, although a previous Gynecologic Oncology Group Phase III study (GOG 92) demonstrated that adjuvant radiotherapy decreases recurrence and prolongs PFS [9,10], it remains unclear whether the addition of concurrent chemotherapy to EBRT is safer and better than RT alone.

The optimal dose of concurrent weekly nedaplatin in patients with invasive cervical cancer treated by primary radiotherapy was investigated in two phase I [14,25] and two phase II studies [26,27]. In these studies, 30–35 mg/m$^2$ nedaplatin for 5–6 weeks was safely administered and was recommended as a standard treatment regimen. In the setting of adjuvant therapy, the optimal dose of concurrent weekly nedaplatin has not been well established because nedaplatin-based adjuvant CCRT has only been evaluated in one phase I study [28], in which the authors recommended 30 mg/m$^2$ nedaplatin for 5 weeks as a standard treatment regimen.

Although the dose of nedaplatin utilized in the current study, 40 mg/m$^2$ nedaplatin for 5 weeks, was slightly higher than that of the previous study [28], nedaplatin-based adjuvant CCRT was well tolerated in our patient population. Grade 3–4 acute toxicities were observed in 64.3% of patients treated with CCRT, which was significantly higher than the proportion observed in the RT-group. This finding is consistent with a previous study that showed that the frequency of acute adverse effects was increased by concurrent chemoradiotherapy [11]. Nevertheless, there were no significant differences in the length of radiotherapy among these treatment groups.

Due to the lack of a controlled clinical study, it is not clear whether concurrent chemotherapy increases the incidence of late toxicity in the setting of adjuvant therapy. In our study, severe late complications were only observed in one patient treated with RT, which may indicate that the addition of concurrent weekly nedaplatin to pelvic RT does not increase late toxicity.

Although retrospective, to the best of our knowledge, this is the first report that has demonstrated significant improvements in recurrence rate, PFS, and OS in patients treated with nedaplatin-based adjuvant CCRT. Risk of recurrence was decreased by 43.7% and 86.8% in the high-risk and intermediate groups, respectively. Importantly, the addition of concurrent nedaplatin-based chemotherapy resulted in fewer local and distant relapses. Consequently, in the intermediate-risk patients, the 3-year overall survival rate for patients receiving CCRT was 100% versus 82.9% for patients receiving RT alone. Moreover, in the high-risk patients, the 3-year overall survival rate for patients receiving CCRT was 88.2% versus 67.6% for patients receiving RT alone, indicating that the risk of death was decreased by 64% by the addition of nedaplatin-based concurrent chemotherapy. Our results are comparable to those of a previous prospective randomized study, GOG 109/SWOG 87-97, which showed the 4-year overall survival of 81% and 71% for high-risk patients receiving cisplatin-based adjuvant CCRT and RT alone, respectively. Correctively, these results indicate that concurrent nedaplatin-based adjuvant chemoradiotherapy can be considered as an alternative to cisplatin-based adjuvant chemoradiotherapy.

In the current study, although the addition of concurrent chemotherapy to pelvic RT resulted in improved survival, a significant number of patients still suffered recurrence and died of their disease, especially those who displayed high-risk prognostic factors. Therefore, to further improve prognosis, novel treatment strategies such as the use of a new cytotoxic agent for concurrent chemotherapy, the use of a biologic agent as a radiosensitizer, or more conformal dose distributions with intensity-modulated RT need to be investigated in future clinical trials.

One limitation of the present study is the relatively small sample size. The recurrence rate, PFS, and OS were significantly improved by the addition of concurrent nedaplatin in the intermediate-risk patients; however, in the patients with high-risk prognostic factors, although OS was significantly improved, the observed improvements in recurrence rate and PFS did not reach statistical significance, mainly because of the small number of patients enrolled. Moreover, due to the retrospective nature of this study, other potential biases may have influenced the results, such as the heterogeneity of the patient population, and selection bias exercised by physicians in determining which patients would be considered for adjuvant CCRT. In addition, the educational level and the socio-economic status of the patients might also have affected patient selection for the treatment scheme.

In conclusion, our data demonstrate that the concurrent use of weekly nedaplatin with pelvic RT improves survival outcome in early-stage cervical cancer patients that display intermediate-risk or high-risk prognostic factors. Given the advantage of patient's tolerance as well as its significant activity, we believe that nedaplatin-based adjuvant chemoradiotherapy is a reasonable treatment option in this patient population. To definitively demonstrate the activity of nedaplatin-based adjuvant CCRT, further investigation in a future randomized controlled trial, such as to compare concurrent nedaplatin versus cisplatin in the setting of adjuvant CCRT, is warranted.

**Conflict of interest statement**
The authors declare that they have no conflicts of interest.

## Acknowledgments

We thank Remina Emoto for providing secretarial assistance.

This work was supported, in part, by a Grant-in-aid for Young Scientists, No 21791554, from the Ministry of Education, Culture, Sports, Science, and Technology of Japan, and a Grant-in-aid for General Scientific Research, No 21390453.

## References

[1] Landoni F, Maneo A, Colombo A, Placa F, Milani R, Perego P, et al. Randomised study of radical surgery versus radiotherapy for stage Ib–IIa cervical cancer. Lancet 1997;350:535–40.
[2] Morley GW, Seski JC. Radical pelvic surgery versus radiation therapy for stage I carcinoma of the cervix (exclusive of microinvasion). Am J Obstet Gynecol 1976;126:785–98.
[3] Perez CA, Camel HM, Kao MS, Hederman MA. Randomized study of preoperative radiation and surgery or irradiation alone in the treatment of stage IB and IIA carcinoma of the uterine cervix: final report. Gynecol Oncol 1987;27:129–40.
[4] Aoki Y, Sasaki M, Watanabe M, Sato T, Tsuneki I, Aida H, et al. High-risk group in node-positive patients with stage IB, IIA, and IIB cervical carcinoma after radical hysterectomy and postoperative pelvic irradiation. Gynecol Oncol 2000;77:305–9.
[5] Inoue T, Morita K. Long-term observation of patients treated by postoperative extended-field irradiation for nodal metastases from cervical carcinoma stages IB, IIA, and IIB. Gynecol Oncol 1995;58:4–10.
[6] Samlal RA, van der Velden J, Schilthuis MS, González González D, Ten Kate FJ, Hart AA, et al. Identification of high-risk groups among node-positive patients with stage IB and IIA cervical carcinoma. Gynecol Oncol 1997;64:463–7.
[7] Delgado G, Bundy B, Zaino R, Sevin BU, Creasman WT, Major F. Prospective surgical–pathological study of disease-free interval in patients with stage IB squamous cell carcinoma of the cervix: a Gynecologic Oncology Group study. Gynecol Oncol 1990;38:352–7.
[8] Fuller Jr AF, Elliott N, Kosloff C, Hoskins WJ, Lewis Jr JL. Determinants of increased risk for recurrence in patients undergoing radical hysterectomy for stage IB and IIA carcinoma of the cervix. Gynecol Oncol 1989;33:34–9.
[9] Rotman M, Sedlis A, Piedmonte MR, Bundy B, Lentz SS, Muderspach LI, et al. A phase III randomized trial of postoperative pelvic irradiation in stage IB cervical carcinoma with poor prognostic features: follow-up of a gynecologic oncology group study. Int J Radiat Oncol Biol Phys 2006;65:169–76.
[10] Sedlis A, Bundy BN, Rotman MZ, Lentz SS, Muderspach LI, Zaino RJ. A randomized trial of pelvic radiation therapy versus no further therapy in selected patients with stage IB carcinoma of the cervix after radical hysterectomy and pelvic lymphadenectomy: a Gynecologic Oncology Group study. Gynecol Oncol 1999; 73:175–6.
[11] Peters III WA, Liu PY, Barrett II RJ, Stock RJ, Monk BJ, Berek JS, et al. Concurrent chemotherapy and pelvic radiation therapy compared with pelvic radiation therapy alone as adjuvant therapy after radical surgery in high-risk early-stage cancer of the cervix. J Clin Oncol 2000;18:1606–13.
[12] Rose PG. Chemoradiotherapy: the new standard care for invasive cervical cancer. Drugs 2000;60:1239–44.
[13] National Comprehensive Cancer Network Clinical Practice Guidelines in Oncology, Cervical Cancer—v.1.2006. http://www.nccn.com/professionals/physician_gls/PDF/cervical.pdf.
[14] Yoshinaga K, Niikura H, Ogawa Y, Nemoto K, Nagase S, Takano T, et al. Phase I trial of concurrent chemoradiation with weekly nedaplatin in patients with squamous cell carcinoma of the uterine cervix. Gynecol Oncol 2007;104:36–40.
[15] Monk BJ, Alberts DS, Burger RA, Fanta PT, Hallum III AV, Hatch KD, et al. In vitro phase II comparison of the cytotoxicity of a novel platinum analog, nedaplatin (254-S), with that of cisplatin and carboplatin against fresh, human cervical cancers. Gynecol Oncol 1998;71:308–12.
[16] Sasaki Y, Shinkai T, Eguchi K, Tamura T, Ohe Y, Ohmori T, et al. Prediction of the antitumor activity of new platinum analogs based on their ex vivo pharmacodynamics as determined by bioassay. Cancer Chemother Pharmacol 1991;27:263–70.
[17] Uehara T, Watanabe H, Itoh F, Inoue S, Koshida H, Nakamura M, et al. Nephrotoxicity of a novel antineoplastic platinum complex, nedaplatin: a comparative study with cisplatin in rats. Arch Toxicol 2005;79:451–60.
[18] Kawai Y, Taniuchi S, Okahara S, Nakamura M, Gemba M. Relationship between cisplatin or nedaplatin-induced nephrotoxicity and renal accumulation. Biol Pharm Bull 2005;28:1385–8.
[19] Fukuda M, Shinkai T, Eguchi K, Sasaki Y, Tamura T, Ohe Y, et al. Phase II study of (glycolate-*O,O'*) diammineplatinum(II), a novel platinum complex, in the treatment of non-small-cell lung cancer. Cancer Chemother Pharmacol 1990;26: 393–6.
[20] Inuyama Y, Miyake H, Horiuchi M, Hayasaki K, Komiyama S, Ota K, et al. Clinical study of *cis*-diammine glycolato platinum, 254-S, for head and neck cancers. Gan To Kagaku Ryoho 1992;19:863–9.
[21] Kato T, Nishimura H, Yakushiji M, Noda K, Terashima Y, Takeuchi S, Takamizawa H, Suzuki M, Arai M, Ota M, et al. Phase II study of 254-S (*cis*-diammine glycolato platinum) for gynecological cancer. Gan To Kagaku Ryoho 1992;19:695–701.
[22] Mabuchi S, Morishige K, Fujita M, Tsutsui T, Sakata M, Enomoto T, et al. The activity of carboplatin and paclitaxel for recurrent cervical cancer after definitive radiotherapy. Gynecol Oncol 2009;113:200–4.
[23] Nakamura Y, Hasegawa M, Hayakawa K, Matsuura M, Suzuki Y, Nasu S, et al. Induction of p53-dependent apoptosis in vivo by nedaplatin and ionizing radiation. Oncol Rep 2000;7:261–5.
[24] Tanaka T, Yukawa K, Umesaki N. Radiation reduces carboplatin sensitivity and enhances nedaplatin sensitivity in cervical squamous cell carcinoma in vitro. Eur J Gynaecol Oncol 2007;28:352–5.
[25] Onishi Y, Nakamura T, Hatae M, Adachi S, Ogasawara T. Phase I study of weekly and radiation therapy for advanced cervical cancer. Proc ASCO 2002;21:111b.
[26] Yokoyama Y, Takano T, Nakahara K, Shoji T, Sato H, Yamada H, et al. Multicenter trial of concurrent chemoradiotherapy with weekly nedaplatin in advanced uterine cervical carcinoma: Tohoku Gynecologic Cancer Unit Study. Oncol Rep 2008;19:1551–6.
[27] Niibe Y, Tsunoda S, Jobo T, Imai M, Matsuo K, Matsunaga K, et al. Phase II study of radiation therapy combined with weekly nedaplatin in locally advanced uterine cervical carcinoma (LAUCC): Kitasato Gynecologic Radiation Oncology Group (KGROG 0501)—initial analysis. Eur J Gynaecol Oncol 2008;29:222–4.
[28] Kodama J, Takemoto M, Seki N, Nakamura K, Hongo A, Kanazawa S, et al. Phase I study of weekly nedaplatin and concurrent pelvic radiotherapy as adjuvant therapy after radical surgery for cervical cancer. Int J Gynecol Cancer 2008;18: 1037–41.
[29] Cox JD, Stetz J, Pajak TF. Toxicity criteria of the Radiation Therapy Oncology Group (RTOG) and the European Organization for Research and Treatment of Cancer (EORTC). Int J Radiat Oncol Biol Phys 1995;31:1341–6.
[30] Whitney CW, Sause W, Bundy BN, Malfetano JH, Hannigan EV, Fowler Jr WC, et al. Randomized comparison of fluorouracil plus cisplatin versus hydroxyurea as an adjunct to radiation therapy in stage IIB–IVA carcinoma of the cervix with negative para-aortic lymph nodes: a Gynecologic Oncology Group and Southwest Oncology Group study. J Clin Oncol 1999;17:1334–5.
[31] Morris M, Eifel PJ, Lu J, Grigsby PW, Levenback C, Stevens RE, et al. Pelvic radiation with concurrent chemotherapy compared with pelvic and para-aortic radiation for high-risk cervical cancer. N Engl J Med 1999;340:1137–43.
[32] Rose PG, Bundy BN, Watkins EB, Thigpen JT, Deppe G, Maiman MA, et al. Concurrent cisplatin-based radiotherapy and chemotherapy for locally advanced cervical cancer. N Engl J Med 1999;340:1144–53.
[33] Keys HM, Bundy BN, Stehman FB, Muderspach LI, Chafe WE, Suggs III CL, et al. Cisplatin, radiation, and adjuvant hysterectomy compared with radiation and adjuvant hysterectomy for bulky stage IB cervical carcinoma. N Engl J Med 1999;340:1154–61.